Journal of Medicinal Chemistry

Article

pubs.acs.org/jmc

Synthesis and Antimitotic and Tubulin Interaction Profiles of Novel Pinacol Derivatives of Podophyllotoxins

Andrés Abad,[†,‡] José L. López-Pérez,*[,†] Esther del Olmo,[†] Luis F. García-Fernández,[§] Andrés Francesch,[§] Chiara Trigili,[∥] Isabel Barasoain,[∥] José M. Andreu,[∥] J. Fernando Díaz,*[,∥] and Arturo San Feliciano[†]

[†]Departamento de Química Farmacéutica, Facultad de Farmacia-CIETUS, Campus Unamuno, Universidad de Salamanca, 37007 Salamanca, Spain

[‡]Departamento de Química, Facultad de Ciencias, Universidad de Los Andes, Mérida, Venezuela

[§]PharmaMar SA, P. I. La Mina, 28770 Colmenar Viejo, Madrid, Spain

[∥]Centro de Investigaciones Biológicas, CSIC, 28006 Madrid, Spain

Supporting Information

ABSTRACT: Several pinacol derivatives of podophyllotoxins bearing different side chains and functions at C-7 were synthesized through reductive cross-coupling of podophyllotoxone and several aldehydes and ketones. While possessing a hydroxylated chain at C-7, the compounds retained their respective hydroxyl group with either the 7α (podo) or 7β (epipodo) configuration. Along with pinacols, some C-7 alkylidene and C-7 alkyl derivatives were also prepared. Cytotoxicities against neoplastic cells followed by cell cycle arrest and cellular microtubule disruption were evaluated and mechanistically characterized through tubulin polymerization inhibition and assays of binding to the colchicine site. Compounds of the epipodopinacol (7β-OH) series behaved similarly to podophyllotoxin in all the assays and proved to be the most potent inhibitors. Significantly, 7α-isopropyl-7-deoxypodophyllotoxin (**20**), without any hydroxyl function, appeared as a promising lead compound for a novel type of tubulin polymerization inhibitors. Experimental results were in overall agreement with modeling and docking studies performed on representative compounds of each series.

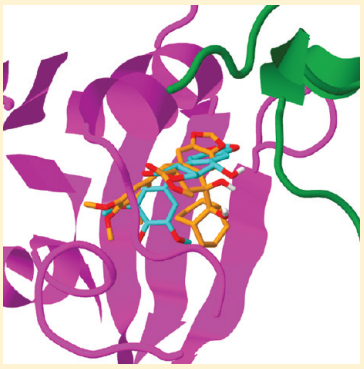

INTRODUCTION

The structural diversity of natural compounds is impressive and covers a broad spectrum of activity against a variety of diseases, including anti-infective, immunomodulation, and neurological disorders, but they have displayed a major impact on cancer chemotherapy. Newman et al.[1] reported that more than 60% of the drugs approved for cancer treatment during 1981−2002 were natural products or derived from them. More recently, Butler has reported on the natural and related compounds, which have been approved or subjected to clinical assays since the beginning of the century.[2,3]

One of those interesting natural compounds in cancer chemotherapy is podophyllotoxin (**1a**, Figure 1), an antineoplastic and antiviral cytotoxic cyclolignan isolated from *Podophyllum* spp. and several species of other genera and families. It is currently used against condiloma acuminata and other venereal warts.[4] In spite of its initial potential as an anticancer drug, human clinical trials were soon abandoned because of its toxicity and severe adverse effects.[5] However, an extensive program of structure−activity optimization at Sandoz resulted in the development and ulterior clinical introduction of two glucoside derivatives of 4′-*O*-demethylepipodophyllotoxin (etoposide (**2a**) and teniposide (**2b**)) and more recently that of etopophos (etoposide phosphate, **2c**, Figure 1), a prodrug designed to overcome the limitations associated with the poor solubility of etoposide.[6,7] Diacylation of the free hydroxyl groups of **2c** led to the dual Topo I and Topo II inhibitor tafluposide (**2d**), which is currently undergoing clinical trials.[8] **2a** is one of the most prescribed anticancer drugs, with good clinical prognosis against several types of cancer, including lung and testicular carcinomas, lymphoma, nonlymphocytic leukemia, and glioblastoma multiforme.[9] As proof of the actual importance of **2a**, it can be verified that this drug and its prodrug **2c** are being currently included in a considerable number of clinical trials of combined anticancer chemotherapy.[10] Continuous efforts on podophyllotoxin modification led to the synthesis and development of several related compounds, as NK611[11] **2e** and GL331 **2f** (Figure 1), which underwent phase II clinical trials.[13] GL331 was more potent than etoposide and showed a promising potential in the treatment of gastric carcinoma, colon cancer, and non-small-cell lung cancer.[14,15] NK611 could be administered orally. Other related compounds displayed anti-inflammatory, antiarthritic,[16] antiviral,[17] and immunosuppressant activities.[18]

From a mechanistic point of view, it has been demonstrated that podophyllotoxin and its related 4′-methoxy congeners act by inhibiting tubulin polymerization through interaction at the

Received: December 30, 2011
Published: May 21, 2012

 © 2012 American Chemical Society

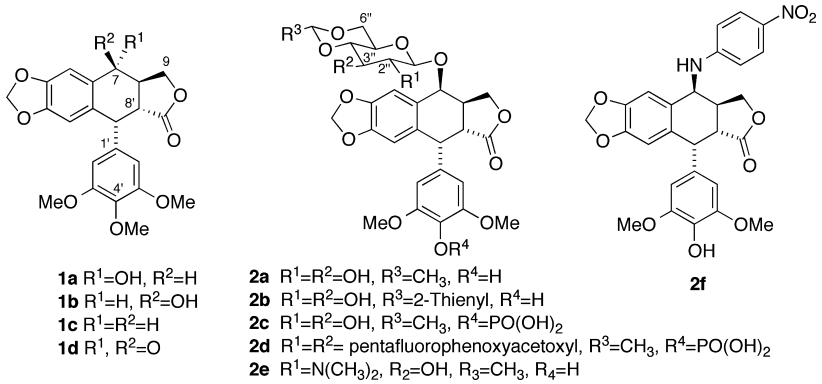

Figure 1. Structures of podophyllotoxins and some related anticancer drugs. Structural numbering is in accordance with the IUPAC nomenclature rules for lignans.[12]

colchicine binding site,[19] whereas a different mechanism is accepted for 4′-demethylepipodophyllotoxin derivatives (compounds **2a**−**f**) which primarily would inhibit DNA topoisomerase II.[20] Recently, some of us have found certain experimental proof on the existence of a third mechanism for a number of podophyllotoxin-derived lignans, which showed induction of neoplastic-cell apoptosis without previous tubulin inhibition.[21] Unfortunately, despite the intensive efforts focused on obtaining better derivatives or analogues, no substance of this family has been found that could outperform the efficacy of podophyllotoxin (**1a**) and deoxypodophyllotoxin (**1c**) for inhibiting microtubule assembly.[22] In addition, podophyllotoxin related compounds retain the typical adverse effects common to most antineoplastic agents, namely, medullar depression, anemia, hair loss, and severe gastrointestinal disturbances, in close correspondence with the potency of their respective cytotoxicities. Therefore, it could be argued that compounds with better affinity for the active site could provide more selective, less toxic, and less adverse effects antineoplastic drugs. Recent reports on thermodynamics of podophyllotoxin-tubulin binding[23] and the design and evaluation of new tubulin inhibitors[24] reveal the current interest in this research field.

The structural features considered fundamental for antitubulin activity of podophyllotoxin derivatives are the trans-fused γ-lactone, the fused dioxole ring, and the almost orthogonal free-rotating 3,4,5-trimethoxyphenyl fragment. On the other hand, for DNA topoisomerase II inhibition, the free 4′-phenol group is crucial while the presence of a bulky free rotating group at the C-7β position would be most favorable.[25] Thus, whereas compounds of the 7-deoxy and 7α-OH (podo) series prove to be good tubulin inhibitors, those bulky derivatives of or related to the β-OH (epipodo) series are as good DNA topoisomerase II inhibitors. Such fair structure−activity relationships point to the C-7 neighboring area as a preferred molecular region for generating structural diversification significant for both types of activity and for the antineoplastic mechanism.[26] Accordingly, with the aim of adding extra fragments that would increase site occupation and could enhance the affinity and selectivity of interaction and could reduce the adverse effects and toxicity of podophyllotoxin-related lignans, we designed several series of novel derivatives that would increase pocket occupation, bearing different side chains and functions at C-7. The series of compounds to be synthesized was mainly constituted of pinacols with either the 7α-OH or the 7β-OH configuration along with several derivatives and analogues. The novelty of this type of structural modifications lies in the fact that these compounds, besides possessing a variable substituent at C-7, simultaneously would retain the α-oriented hydroxyl group of podophyllotoxin (podo-like, **1a**), are expected to maintain the anti-tubulin activity, or can change toward the β-oriented hydroxyl of epipodophyllotoxin (epipodo-like, **1b**). Furthermore, adequate 7-OH derivatization and selective O-demethylation at 4′ could also lead to 7α,7β-disubstituted podophyllotoxins configuring a new scaffold for potential DNA-topoisomerase inhibitors.

The McMurry reaction, based on the use of low-valent titanium catalysts generated in situ from $TiCl_3$ or $TiCl_4$, constitutes the most common procedure to attain the reductive coupling or cross-coupling of aldehydes and/or ketones in pinacol synthesis.[27] On this basis, we assayed different procedures and conditions related to the McMurry methodology because this methodology could lead to pinacols but also to olefins by simple controlling of reaction conditions. According to the results found in the prospective assays of podophyllotoxone cross-coupling, we selected the system $TiCl_4$/Zn dust/dry THF and defined the temperature and time conditions for which acceptable results were obtained. Under such conditions appropriate proportions of podo and epipodo derivatives were produced independent of the presence of overreduced products, which were easily separated by chromatography from the desired pinacols. Under adequate temperature control, the procedure was also employed to prepare several olefin derivatives because initial attempts based on the Wittig reaction were very inefficient for the alkylidenation of podophyllotoxone. The structures of the compounds reported here were generally established through the analysis of 1D and 2D NMR spectra, complemented in several cases with X-ray diffraction analysis and/or some molecular modeling calculations. ^{1}H and ^{13}C chemical shifts of representative compounds were fully assigned using COSY, HMQC, and HMBC 2D NMR correlations.

Important features associated with the compounds included in this report are the retention or improvement of the antineoplastic cytotoxicity levels and the fair antimitotic activity displayed by most of them. Pinacols and 7α-alkyl derivatives of podophyllotoxins (Table 1) constitute novel classes of podophyllotoxin related lignans, being highly cytotoxic against cultured cancer cells. Consequently, they could open a route for the development of new and more selective anticancer agents.

■ RESULTS

Chemistry. The starting podophyllotoxin (**1a**) was isolated from commercial *Podophyllum* resin and transformed into

podophyllotoxone **1d** through a well documented and previously reported procedure.[28] The desired hybrid pinacol derivatives of podophyllotoxins **4**−**17** were synthesized through McMurry type condensations[29−31] of podophyllotoxone (**1d**) with a variety of carbonyl compounds including several aldehydes and ketones (Figure 2). These reactants were

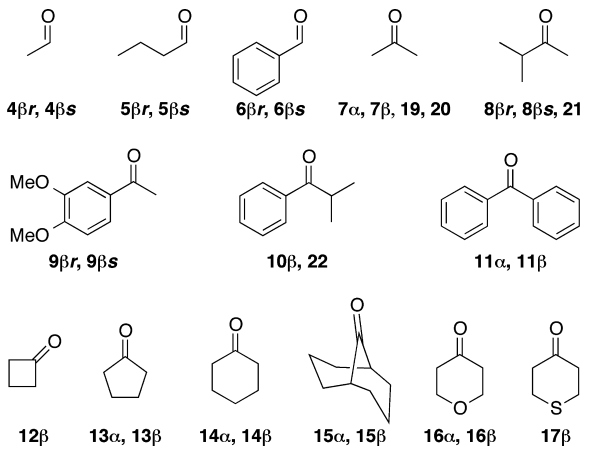

Figure 2. Carbonyl compounds used as reagents in the synthesis of pinacol derivatives and related compounds.

selected to obtain a preliminary exploratory series with some structural diversity. The α/β codes employed to denominate most compounds in this paper refer to the actual configuration of the hydroxyl group located at C-7 that can be oriented as in podophyllotoxin (**1a**, 7α-OH) or as in epipodophyllotoxin (**1b**, 7β-OH) and is also referred to in this paper as the podo and epipodo series, respectively. The codes ***r***/***s*** refer to the respective *R*/*S* absolute configuration of the new stereocenter generated in the course of reductive cross-coupling, when the reaction is carried out with a nonsymmetrically substituted carbonyl substrate (Figure 2, Table 1). Syntheses of pinacol and alkene derivatives of podophyllotoxin are outlined in Scheme 1. Summarily, ketolignan **1d** was cross-condensed with an aldehyde or a ketone in the presence of $TiCl_4$/Zn dust in dry THF under the conditions and temperature described in the Experimental Section. This coupling procedure proved to be an efficient method for the synthesis of small amounts of lignan-ketone/lignan-aldehyde hybrids, including both pinacol and olefin classes of derivatives. Nevertheless, yields were usually not too high, since the desired pinacols reduced lignans as podophyllotoxin **1a**, epipodophyllotoxin **1b**, and deoxypodophyllotoxin **1c** were formed as secondary products during the reaction, due to the Zn excess usually employed. Furthermore, as expected, pinacol dimers derived from the aldehyde (ketone) autocondensation were also formed.

The $TiCl_4$−Zn catalyzed reductive cross-coupling at −10 °C of ketolignan **1d** and symmetrically substituted carbonyl compounds (Figure 2) afforded a mixture of two pinacols, one of the epipodo and one of the podo series. Under the conditions used, the epipodo derivative was formed in a higher ratio (7:3 approximately) compared with the podo series. In the case of using aldehydes or nonsymmetric ketones, only those epipodo pinacols were obtained in appreciable yield. The desired compounds were in general isolated from the reaction crude through flash chromatography and purified by subsequent recrystallization. Traces of those corresponding podo epimers were also detected between the mixtures of the residual starting ketone **1d** and the main reaction byproducts **1a**, **1b**, and **1c**. Their isolation and purification were not attempted in most cases because of their scarce amounts and the complexity of the reaction mixtures.

As it has been stated, the olefination of ketolignan **1d** by the attempted Wittig reaction in different conditions did not work. It has also been reported that **1d** is inert toward Grignard reagents and does not readily react with other nucleophiles because of the presence of the neighboring electron-rich aromatic system.[32] On the other hand, the McMurry reaction worked well and led to the desired C-7/C-1″ olefin hybrids, along with variable amounts of corresponding epipodopinacols, provided the reaction was carried out under reflux for 24 h. However, the increase of the reaction time in order to decrease or to avoid the pinacol presence usually led to unresolvable mixtures of degraded lignans. In the assayed cases, repeated crystallizations of the crude reaction products provided the olefins **19**, **21**, and **22** in 40−50% yield of pure compound. The ulterior reduction of olefin **19** with H_2-Pd/C afforded the corresponding dihydrogenated compound **20** in >95% yield, with the α-oriented side chain at C-7 (Scheme 1). The previously known methylidene derivative **18** was obtained by the Takai reaction as described in the literature.[33]

Pinacol derivatives of **1d** obtained through cross-coupling with symmetric ketones constitute an interesting group of molecular structures with four contiguous stereocenters whose stereochemical aspects can easily be correlated with those of

Scheme 1. Synthesis of Pinacol, Olefin, and Dihydro Derivatives[a]

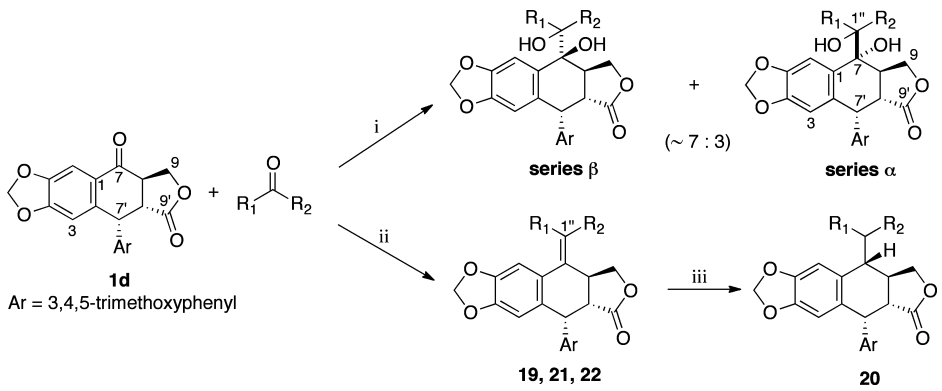

[a]Reagents and conditions: (i) $TiCl_4$, Zn dust, dry THF, −10 °C, 4 h; (ii) $TiCl_4$, Zn dust, dry THF, 60 °C, 24 h; (iii) H_2-Pd/C, MeOH, 1 atm, 24 h.

known natural *Podophyllum* lignans. However, when aldehydes or nonsymmetrically substituted ketones were employed in the cross-coupling reaction, one additional stereocenter is created at the side chain during the reaction. In such cases, the elucidation of the stereochemical aspects for completing the structure assignment was not too obvious. In several cases, 2D NMR correlations (HMBC, HMQC, and ROESY) and other experiments were needed for ascertaining the absolute configurations of the new stereocenter. Some diagnostic connectivities between the C-7 side chain and the lignan fragment were particularly analyzed. The C-7 configuration of pinacols was deduced from a comparison of ^{13}C chemical shifts of the oxygenated pinacol carbons and from particular ROESY results for each compound. Thus, it was observed that chemical shifts for C-7 in the podo series (pseudo-equatorial 7α-OH) of pinacols are several ppm higher than those found for their respective epipodo (pseudo-axial 7β-OH) analogues. As an example, in the case of the epimeric compounds **14*α*** and **14*β***, the C-7 signals in their ^{13}C NMR spectra appear at δ 88.0 and 78.7 ppm, respectively. This finding is in agreement with those data found for podophyllotoxin (72.8 ppm) and epipodophyllotoxin (67.0 ppm).[34] The study of ROESY correlations and the distances derived from theoretical models (complementary calculations not reported here) enabled the definitive stereochemical assignments shown in Table 1 for pinacol derivatives. In compounds of the 7β-OH series, ROE correlations were observed between signals associated with side chain protons and those of the methines in the trimethoxyphenyl group, as well as with that of H-8. Correspondingly, in the case of the 7α-OH analogues, ROE correlations were detected for signals of the side chain protons with those assigned to H-9 and H-8′ in the lignan core. As an example, for compound **14*β*** a ROE cross-signal correlated the 3,5-methoxy groups (δ 3.73 ppm) with some cyclohexyl protons (δ 1.55−1.68 ppm), while another strong ROE correlation was observed between cyclohexyl signals and that of H-8 (δ 2.63 ppm, ddd). Both correlations could only agree with the pseudo-equatorial disposition of the cyclohexyl fragment, and consequently, this epimer must belong to the 7β-OH series. In the case of compound **14*α***, a ROE correlation was observed between the H-8′ signal (δ 3.50 ppm, dd) and a multiplet centered at δ 1.7 ppm assigned to cyclohexyl protons, while an additional ROE correlation was observed between the same cyclohexyl signal and that at δ 3.46 ppm (H-9β, dd). This correlation can only agree with the pseudo-axial disposition of the cyclohexyl substituent in the podo 7α-OH series.

In the cases of olefins **21** and **22**, the assignment of the double bond configuration was also based on ROESY correlations. In both cases, only one stereoisomer, with the *Z* configuration, was isolated from the reaction product. Thus, in the case of compound **22**, the strong ROE correlation observed between the signal at δ 3.42 ppm, unequivocally assigned to H-8, and that of the isopropyl methine (δ 2.96 ppm, m) clearly indicated the *Z* configuration of the olefin. This assignment was in complete agreement with the model obtained after a molecular modeling study, from which a distance of 2.029 Å between both protons was derived. Additionally, as a confirming observation, a strong shielding of the H-6 signal (δ 6.59 ppm, s) was produced because of the proximity and the spatial orientation of the trimethoxyphenyl group. In fact, the calculated molecular model showed a distance of 3.029 Å between H-6 and the centroid of the trimethoxyphenyl group. Similarly, for compound **21** two clear ROE correlations between H-6 (δ 6.88 ppm, s) and the isopropyl methine (δ 3.4 ppm, m) and also between H-9β (δ 4.10 ppm, dd) and the olefinic methyl (δ 1.65 ppm, s) were observed. Both ROE correlations allowed us to propose the *Z* configuration for this compound. Structures of several compounds, including **8*βr***, **14*β***, and **21**, were confirmed by X-ray diffraction analysis (data not shown).

Biological Results: Cell Growth Inhibition. Cyclolignan derivatives reported here were evaluated in vitro[35] for their antiproliferative activity against 3−13 different lines of human cancer cells. The GI_{50} values for three selected cell lines, A-549 (lung carcinoma), HT-29 (colon carcinoma), and SK-BR3 (breast carcinoma), are summarized in Table 1 (other GI_{50} values are given in Supporting Information). The antineoplastic drug doxorubicin was used as reference standard. Cytotoxicity values for podophyllotoxin (**1a**) and epipodophyllotoxin (**1b**) are included in Table 1 for comparative purposes.

As can be seen in Table 1, the compounds were in general fairly cytotoxic, with GI_{50} values under the micromolar level, while some of them displayed values in the nanomolar range close to, or even better than, those of the reference lignan **1a** or **1b** and doxorubicin. Some important SARs can be deduced from these results. First, it is interesting to note that the introduction of relatively large and bulky substituents at position C-7 did not cause a considerable loss of activity. In general, though in contrast with the natural lignans podophyllotoxin (**1a**, GI_{50} = 12 nM) and epipodophyllotoxin (**1b**, GI_{50} = 60 nM), pinacol derivatives of the 7β-OH (epipodo) series showed greater cytotoxicity than their corresponding 7α-OH (podo) analogues. This fact can be observed for the pairs of epimers **11*β*/11*α***, **13*β*/13*α***, and **14*β*/14*α*** and much more significantly for the pairs **16*β*/16*α*** and **15*β*/15*α*** for which the potency ratio attains up to more than 2 and 3 orders of magnitude, respectively. Additionally, comparison of activity data for compounds **14*β*** and its 8′-epimer, the picropodolactone **14*β*p**, confirms that the transformation of a *trans*-lactone into a *cis*-lactone implies a substantial loss of activity, in agreement with the information reported in the literature.[36] Similarly, in the case of ketals **4*βr*** and **4*βs***, considered in comparison with the pinacol derivative **5**, the masking of the pinacol hydroxyl groups through ketalization appears to diminish the cytotoxicity by 1 order of magnitude. Finally, it is worth highlighting that the formal change of pinacols to the corresponding olefins produces a fair loss of cytotoxicity (**7*α*/7*β***, **8*βr*/8*βs***, and **10*β*** vs **19**, **21**, and **22**, respectively), while the hydrogenation of the olefin **19** leads to a significant increase of almost 2 orders of magnitude in the cytotoxicity of the 7α-isopropyl derivative **20**.

Cell Cycle Studies. In this assay A-549 nonsmall lung carcinoma cells were incubated for 20 h with ligands at concentration ranging from 1 nM to 100 μM and the percent of cells in each phase of the cell cycle was determined by flow cytometry. Controls were done with untreated cells or treated with drug vehicle DMSO. The results for a number of representative compounds are graphically shown in Figure 3, while the complete tabulated quantitative data are given in Supporting Information. It can be noted that all the compounds tested in this assay behaved similarly to the parent drug podophyllotoxin **1a**, though with fair differences in the concentration levels necessary for each compound to accumulate over 70−80% cells in G2/M arrest. As in the above-mentioned studies, compounds with the 7β-hydroxy/7α-(1-hydroxyalkyl) configuration were fairly more effective than

Table 1. Selected Cytotoxicity Data (GI_{50} ± SD, nM) for Pinacol, Alkylidene, and Alkyl Derivatives of Podophyllotoxins against Human Neoplastic Cell Lines[a]

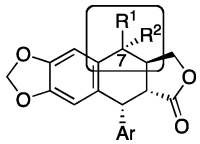

Compound	Position C-7	A-549	HT-29	SK-BR3
1a		**12**	**12**	nt
1b		**60**	**60**	nt
4β*r*		6220 ±562	5230 ±443	5870 ±126
4β*s*		6020 ±526	6560 ±456	6140 ±786
5β*r*		279 ±12	404 ±75	288 ±8
6β*r*		2030 ±15	2510 ±413	2430 ±9
7α		1480 ±564	659 ±43	511 ±65
7β		577 ±61	598 ±83	457 ±24
8β*r*		254 ±6	204 ±2	181 ±7
8β*s*		1150 ±27	1730 ±87	1030 ±70
9β*r*	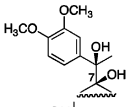	2620 ±65	4750 ±126	4990 ±345
10β		139 ±5	159 ±16	148 ±15
11α		874 ±68	528 ±20	524 ±36
11β		376 ±25	281 ±32	313 ±57
12β		191 ±18	198 ±18	219 ±40
Doxorubicin HCl		**60.3** ±5.6	153 ±4.9	**65.5** ±8.6

Compound	Position C-7	A-549	HT-29	SK-BR3
13α		1690 ±356	2720 ±315	2420 ±154
13β		444 ±12	451 ±8	439 ±29
14α	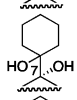	547 ±71	859 ±13	610 ±24
14β		**90.8** ±1.3	**97.5** ±4.6	**64.9** ±2.8
14βp*		3620 ±70	2900 ±38	1250 ±61
15α	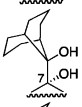	5680 ±6	6420 ±85	6720 ±41
15β	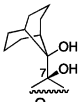	**6.39** ±0.15	**5.14** ±0.50	**7.39** ±0.6
16α		8920 ±317	15440 ±491	8010 ±140
16β	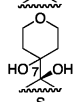	**29.0** ±1.1	**26.8** ±0.3	**25.9** ±0.4
17β		3320 ±213	2620 ±53	1780 ±187
18		**28.1** ±5.0	**78.1** ±7.2	**66.8** ±6.6
19		6440 ±477	8280 ±386	3780 ±82
20		**79.5** ±9.0	**83.1** ±1.4	**84.1** ±3.0
21		7700 ±137	10200 ±221	4530 ±141
22		6210 ±326	11400 ±582	14300 ±589

[a]Cytotoxicity results are expressed as GI_{50} values, the compound concentrations producing a 50% cell growth inhibition, and represent the mean ± SD of three independent experiments. Values under 100 nM are boldfaced for an easier comparison. Data for compounds **1a** and **1b** were taken from our previous research.[37] The asterisk (*) indicates compound with the epimeric 8′α-H configuration (cis-fused/picropodolactone).

their corresponding epimers, and the most active compounds **20** and **15*β***, which were also most cytotoxic (GI_{50} of 80 and 6 nM, respectively), induced the G2/M arrest at concentrations 1 order of magnitude lower than the antimitotic reference drug **1a**. On the other hand, as expected in order to attain a similar result, the epimeric compound **16*α*** needed a 100 μM concentration level, 2 orders of magnitude higher than podophyllotoxin.

Microtubule Assembly Inhibition. We tested if these compounds were able to depolymerize cellular microtubules in

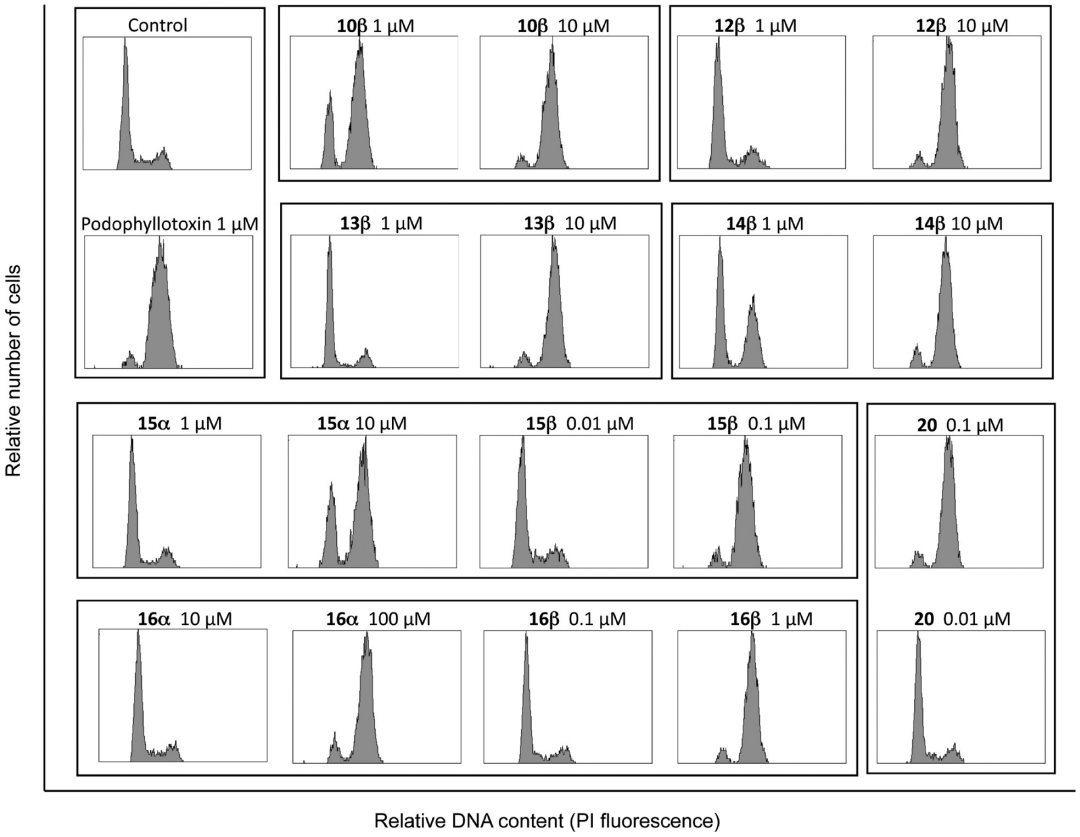

Figure 3. Cell cycle histograms of A-549 cells untreated or treated with podophyllotoxin (**1a**) and its derivatives. Cells were incubated for 20 h at concentrations ranging from 1 nM to 100 μM ligands. The lower ligand concentration that arrests cells in the G2/M phase is depicted.

the same way as podophyllotoxin does. Treatment of A-549 cells for 20 h with different concentrations of **1a** and several selected derivatives led to a complete depolymerization of the microtubule cytoskeleton. Some cells were micronucleated, and there were cells arrested in prometaphase with a ball or rosette of condensed DNA and no mitotic spindle, which is a type IV spindle.[38] With these compounds mitotic arrest was accompanied by net microtubule depolymerization. The effects of the epimers **16*β*** and **16*α*** on the microtubule array of A-549 cells are shown in Figure 4. As can be seen, both compounds were able to attain a similar degree of depolymerization but with a fair difference in potency in favor of compound **16*β***, which was approximately 200-fold more active than **16*α***. Similar results were obtained with **15*β*** and **15*α*** epimers (Supporting Information figures). Podophyllotoxin (**1a**) and the rest of the tested compounds behaved similarly, and pictures can be examined in Supporting Information. 2 μM **10*β***, 5 μM **12*β***, 5 μM **13*β***, 2 μM **14*β***, 20 μM **15*α***, 0.05 μM **15*β***, 100 μM **16*α***, 0.5 μM **16*β***, 0.05 μM **20**, and 2.5 μM podophyllotoxin (**1a**) completely depolymerized the microtubule network of A549 cells. These results correlate quite well with those obtained in tubulin assembly experiments.

On top of that, the degree of tubulin polymerization was evaluated through pellet mass formation in the presence of stoichiometric and semistoichiometric concentrations of the evaluated lignans. Such results, not shown, served to confirm the actual inhibition power for most of the compounds assayed, while several of them displayed effects higher than podophyllotoxin (**1a**), used as positive control. Interestingly and in parallel with the cytotoxicity values shown in Table 1, those compounds of the 7α-OH series appeared to be less

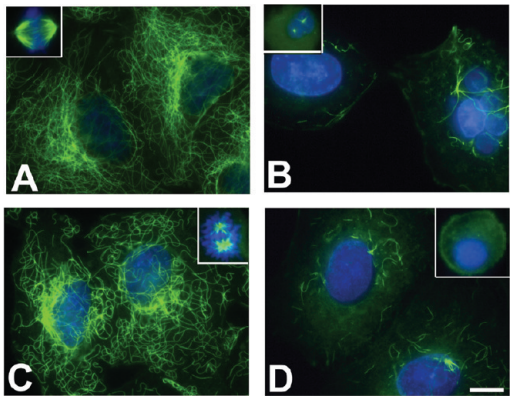

Figure 4. Effects of compounds **16*β*** and **16*α*** on the microtubule array of A-549 lung carcinoma cells. A-549 cells were incubated for 20 h with the ligands or drug vehicle: (A) control; (B) 0.5 μM **16*β***; (C) 50 μM **16*α***; (D) 100 μM **16*α***. Microtubules (green) were stained with α-tubulin antibodies, and DNA (blue) was stained with Hoechst 33342. Insets are mitotic spindles from the same preparation. The scale bar represents 10 μm. All panels and insets have the same magnification.

potent than those of the 7β-OH series (**15*α***, **16*α*** vs **15*β***, **16*β***, respectively). Further experiments to depict inhibition curves (Figure 5) and to determine GI_{50} values confirmed this observation, showing the higher inhibitory power ($GI_{50} < 1$ μM) found for compounds **20** and **15*β***. The 50% inhibitory ligand concentration of tubulin assembly was determined with a centrifugation assay that measured the decrease in the concentrations of assembled microtubules in the presence of

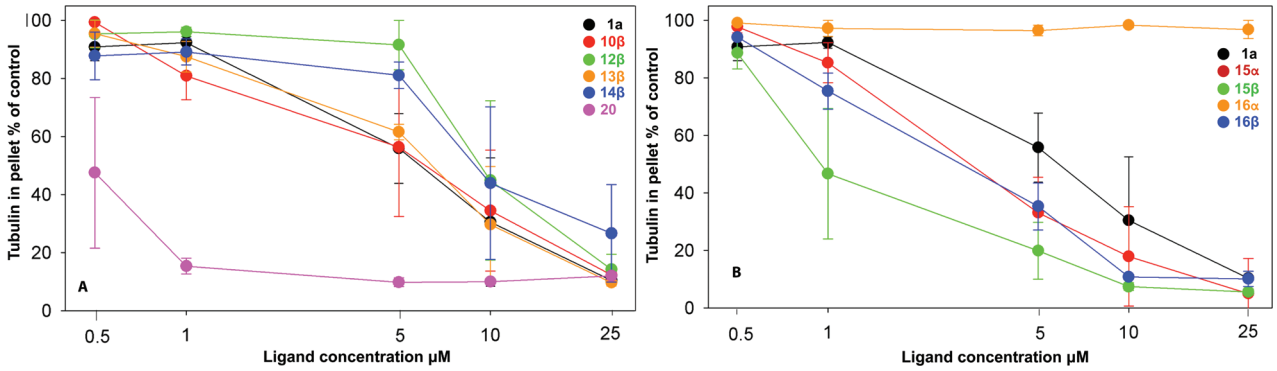

Figure 5. Inhibition of tubulin assembly by lignan derivatives: (A) podophyllotoxin (**1a**), **10*β***, **12*β***, **13*β***, **14*β***, and **20**; (B) podophyllotoxin (**1a**), **15*α***, **15*β***, **16*α***, and **16*β***.

different concentrations of samples. Quantitative data are given as Supporting Information.

Binding Displacements. To complement the above research and to confirm the assumed mechanism for these compounds, related to the interaction at the colchicine site of tubulin, another experiment was performed. Most compounds were assayed for their ability to displace MTC [2-methoxy-5-(2,3,4-trimethoxyphenyl)-2,4,6-cycloheptatrien-1-one], a commercial reversible tubulin ligand, from its binding at the colchicine site.[39,40] The results for podophyllotoxin (**1a**), the most potent (**20**), and one less potent (**16*α***) inhibitor are graphically shown in Figure 6 as representative examples. It can

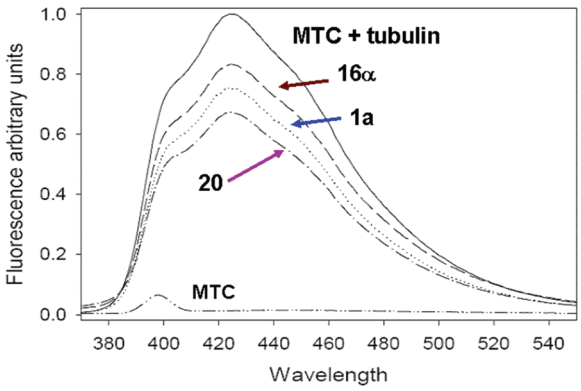

Figure 6. Displacement of MTC from the colchicine binding site by lignan derivatives: fluorescence emission spectra of 10 μM MTC [2-methoxy-5-(2,3,4-trimethoxyphenyl)-2,4,6-cycloheptatrien-1-one] and 10 μM tubulin in 10 mM sodium phosphate and 0.1 mM GTP buffer, pH 7.0, and in the presence of 20 μM compounds **16*α***, **1a**, and **20**. Bottom line is fluorescence emission spectrum of 10 μM MTC in the same buffer.

be readily observed that **1a** displays an intermediate MTC displacement in comparison with compounds **16*α*** and **20**. In its free state MTC (10 μM) under excitation at 350 nm did not show any appreciable level of fluorescence (bottom line). Once tubulin was added (10 μM), fluorescence appeared (upper continuous line). Then the fluorescence level decreased by 35% if **20** (20 μM) was added, by 25% if the reference drug **1a** was added, and by only 15% if **16*α*** was added. The small fluorescence decrease produced by compound **16*α*** could be nonspecific. We cannot rule out potential quenching or allosteric effects. As expected, these results correlate well with those observed in the tubulin assembly inhibition tests.

Molecular Modeling. Studies were performed on the basis of a model of interaction complex between tubulin and podophyllotoxin reported by us,[41] resulting from refined calculations on the previously published crystalline complex.[42] Compounds to be analyzed were submitted to a conformational MMFF force field optimization implemented in Spartan 08[43] to calculate their tubulin interactions with AUTODOCK.[44] Docking of 7*β*-OH derivatives led to energetically and geometrically adequate results for all those analyzed compounds, particularly for those more cytotoxic and more potent tubulin polymerization inhibitors, compounds **15*β***, **16*β***, and **20** (Figure 7D or Figure 7E, Figure 7C, and Figure 7H, respectively). Good results were also observed for compounds with a bulky substituent at C-7*α* and displaying a modest cytotoxicity. Contrarily, compounds with a large or bulky substituent at C-7*β*, as in the cases of compounds **11*α*** (7*β*-diphenylmethyl) and **16*α*** (7*β*-tetrahydropyran-4-yl), failed to dock at the colchicine site of tubulin. Similarly, large 7-alkyllidene derivatives such as compound **22** also failed to dock in tubulin, while the smaller isopropylidene derivative **19** attained the docking, though with a fair displacement of the *γ*-lactone ring from the usual four-ring coplanarity of trans-fused podolignans. Other observations related to the modeled interaction of these lignans with tubulin were of particular interest. Compound **15*β*** led to two different poses of similar energy, one close to and the other rotated about 30° apart from the original podophyllotoxin docking orientation (Figures 7D and 7E). Among the lesser cytotoxic products, the epimeric acetonides **4*βr*** and **4*βs*** were also analyzed. The structural difference between both compounds consisted only of the change in the absolute configuration at the alfa position (1″) in the side chain, and as could be expected, it showed very similar cytotoxic potencies and passed successfully the filtering of accommodation in tubulin. Most surprisingly, the *S* acetonide was automatically placed in a more distant orientation than the one expected in the tubulin pocket. As shown in Figure 7F and Figure 7G, the poses for both epimers are practically inverted in relation to the dioxole/dioxolane rings while the fused tetracyclic system and the trimethoxyphenyl fragment of **4*βs*** were displaced with respect to those of podophyllotoxin and acetonide **4*βr***. Figure 7I and Figure 7J represent two orientations of the docked pyrane derivative **16*β*** with identification of the neighboring tubulin amino acids (3.5 Å apart from the ligand). In Figure 7, the lipophilic nature of the tubulin region around the trimethoxyphenyl fragment (*β*-unit of tubulin) can be observed while the possible hydrogen bond interactions of the pinacol function with the hydroxyl group of threonine-163 (*α*-unit of tubulin) are also indicated.

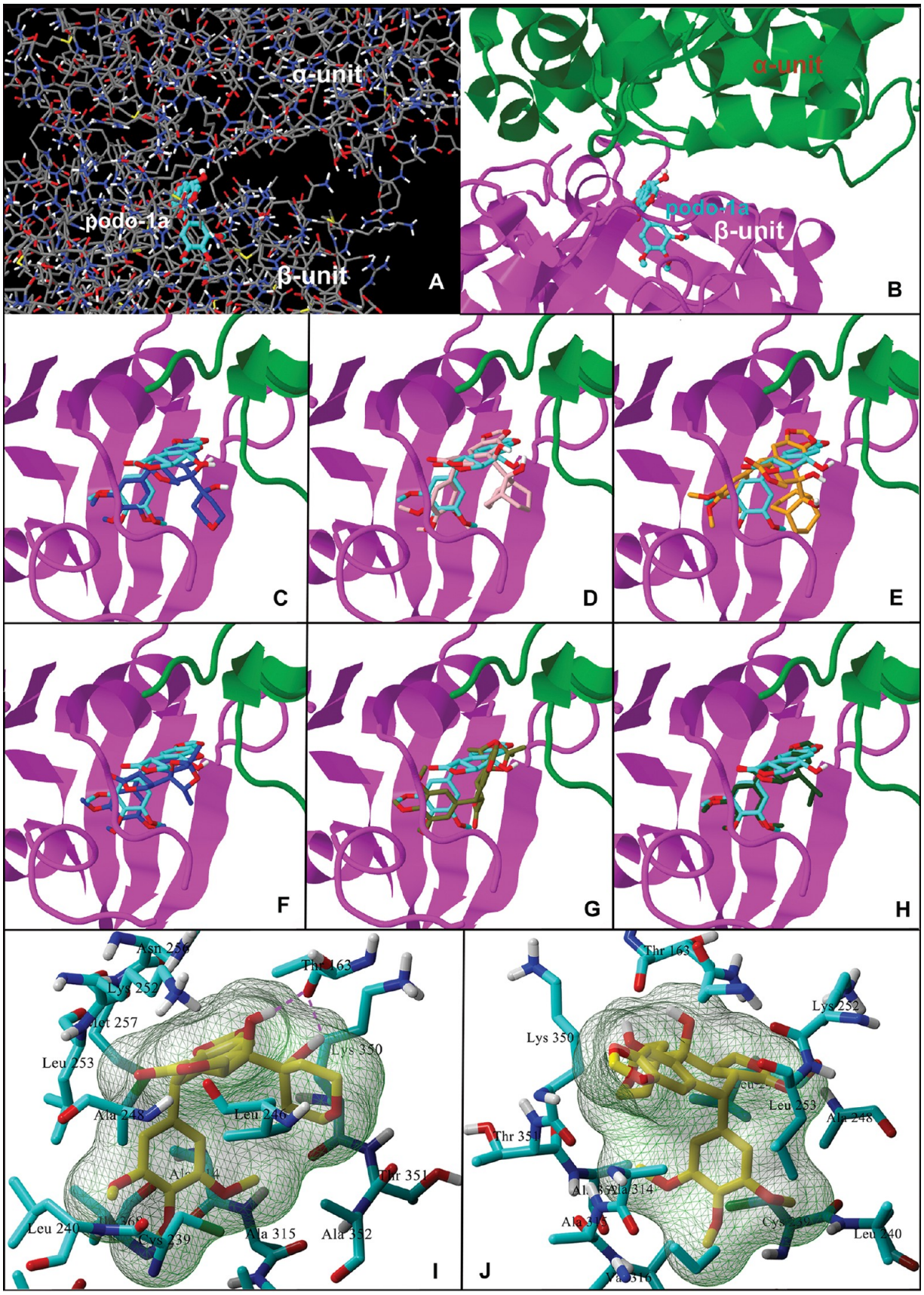

Figure 7. Calculated docking of podophyllotoxin (**1a**, light blue) represented in two different forms and orientations (A, B) to show the probable route of access to the active site between the *α*- and the *β*-tubulin units, and comparative docking of **1a** with several representative polymerization inhibitors, **16*β*** (C), **15*β*** (D, E) (two permitted poses of **15*β***), the ketals **4*βr*** (F) and **4*βs*** (G), the isopropyl derivative **20** (H). Also shown are the amino acid residues of tubulin around the docked inhibitor **16*β*** (I, J). Pink dotted lines indicate H-bonds of pinacol-Thr163 (I).

Table 2. Experimental and Calculated Data Related to the Antineoplastic Antimitotic Activity of Representative Lignan Derivatives

compd	A-549, GI_{50} (nM)	tubulin polymerization inhibition at 1 μM (%)	MTC-binding displacement (%)	docking energy[a] (kcal/mol)
1a	12	7.0	25	−9.2
11α	874	nd	nd	failed
15α	5680	12.0	15	failed
15β	6.39	45.1	nd	−9.2
16α	8920	2.8	nd	failed
16β	29.0	21.1	nd	−10.7
19	6440	nd	nd	−9.0
20	79.5	84.5	35	−10.0
22	6210	nd	nd	failed

[a]From AUTODOCK calculations. nd: not determined.

In order to facilitate a more complete comparison, Table 2 shows the values of cellular cytotoxicity, tubulin polymerization inhibition, and ability to dock in tubulin for representative compounds. Comparable experimental and calculated data for most compounds seem to be in global agreement, with some exceptions that could be interpreted taking into consideration the expected influences of the size of the substituent at C-7 and the degree of site occupation on the respective docking energy. The most prominent exception that deserves further study corresponds to compound **15α**, which showed GI_{50} cytotoxicity above 5 μM and failed to be docked into the active site while being able to inhibit tubulin polymerization and to displace MTC from its binding site. As can also be observed, the most stable conformer of the compounds with a GI_{50} higher than 1 μM failed to be adequately docked into tubulin using the AUTODOCK.2 software, with the exception of olefin **19**.

DISCUSSION AND CONCLUSIONS

In relation to the antineoplastic cytotoxicity of pinacols (Table 1), it had already been mentioned that 7β-OH epimers were significantly more potent than their corresponding 7α-OH analogues. This fact would mean that the size and orientation of the substituent at C-7 should have more importance for the activity than the nature or type of function located at that position. This statement would be reinforced by the higher cytotoxicity showed by compound **20**, without any hydroxyl group at C-7 or its side chain.

The assays and studies that focused on the mechanism of action of these series of compounds have demonstrated a global parallelism between cytotoxicity, cell cycle arrest, and tubulin polymerization inhibition (Figures 4 and 5 and Supporting Information), as well as the proportional displacement of MTC from the colchicine binding site (Figure 6) by those compounds tested. Additionally the compounds assayed behaved similarly to podophyllotoxin (**1a**) in arresting the cellular cycle of A-549 cells at the G2/M phase, with differences in potency only (Figure 3).

In summary, we can conclude that pinacol derivatives obtained from podophyllotoxone (**1d**) retain or even enhance the global antimitotic or antitubulin properties of podophyllotoxin (**1a**) and that the two main series evaluated, whose compounds belong to the epipodophyllotoxin series [7β-OH/7α-(1-hydroxyalkyl) substitution], were fairly more potent than their corresponding C-7 epimers (podophyllotoxin series). Regarding the influence on the activity of the exocyclic $\Delta^{7(1'')}$-olefins, the scarce number of compounds evaluated does not permit any sure conclusions. Nevertheless, it can be argued that the presence of a dialkyl substitution at C-1″, while adding steric tension and conformational deformation around the C-7 zone, fairly decreases the antimitotic activity, as shown for the olefinic derivatives **19**, **21**, and **22**. On the other hand, it seems very important to highlight that a simple hydrogenation of the isopropylidene derivative **19**, a comparatively poor antimitotic within the group of lignans considered in this research, has led to 7α-isopropyldeoxypodophyllotoxin (**20**), which was the most potent tubulin polymerization inhibitor of these series. Very interestingly, compound **20** has no functional group in the side chain attached to C-7. This observation has presented an unexpected structural alternative for designing new and probably more potent tubulin polymerization inhibitors, also based on the observation of the rather lipophilic nature of the unoccupied region in the active site. Virtual docking calculations being recently initiated on several structure proposals with an increased active site occupation, compared to compound **20**, confirm such hypothesis. The experimental chemical work is now focused toward the selective 4′-O-demethylation of those 7α-hydroxy-7β-(1hydroxyalkyl) (podophyllotoxin-like series) derivatives to be evaluated as potential DNA Topo II inhibitors.

EXPERIMENTAL SECTION

Chemistry. Melting points were determined on a Büchi 510-K melting point apparatus and are uncorrected. Optical rotations were recorded on a Perkin-Elmer 241 polarimeter in chloroform solution and UV spectra on a Hitachi 100-60 spectrophotometer in ethanol. IR spectra were recorded (KBr, 1%) in a Nicolet Impact 410 spectrophotometer. ^{1}H, ^{13}C NMR, COSY, HMQC, and HMBC were recorded on Bruker AC 200 (200 MHz) and Bruker DRX 400 (400 MHz) instruments. Silica gel 60 (Merck, 230−400 mesh) was used for flash chromatography. Precoated silica gel plates (Merck, Kieselgel 60 F254, 0.25 mm) were used for TLC analysis. For EIMS and HRFABMS analysis, a VG-TS250 mass spectrometer (70 eV) was used. Elemental analysis results were obtained with a LECO CHNS-932 instrument (see Supporting Information). Before biological testing, compound purity was evaluated by reversed-phase HPLC. HPLC analysis was performed using an Agilent 1100 series equipped with a Synergy Max-RP C12, 250 mm × 4.6 mm column, with gradient H_2O + 0.1% TFA/CH_3CN + 0.1% TFA from 45% to 85% organic in 45 min and from 85% to 100% organic in 5 min, a flow rate of 0.6 mL/min, and UV detection at 254 nm. From HPLC data, the percentage purity is given for each compound. All biologically evaluated compounds are >95% chemically pure as measured by HPLC.

General Procedure for the Preparation of Compounds 4−22. *Protocol A.* To a suspension of zinc dust (1.9 g, 29 mmol) in dry THF (20 mL) under argon at −20 °C, commercial $TiCl_4$/THF (1:2) (2.43 g, 7.3 mmol) was added slowly. After 30 min, once the mixture attained room temperature, podophyllotoxone (**1d**, 200 mg, 0.485 mmol, amount used in every experiment) and the ketone or aldehyde (0.97 mmol) were added, and the mixture was maintained with stirring in the range from −20 °C to −10 °C during 4 h. The reaction was quenched by addition of 2 N HCl (30 mL), and extraction was with EtOAc. The sample was washed until neutral pH was obtained and then dried with Na_2SO_4, and the solvent was removed under reduced pressure. The crude product was purified by column chromatography on silica gel with *n*-hexane/EtOAc and crystallization. In addition to the desired product(s), podophyllotoxin (**1a**) (10−20%), deoxypodophyllotoxin (**1c**) (15−20%), and epipodophyllotoxin (**1b**) (1−2%) were obtained in general as byproducts.

Protocol B. The catalyst was prepared as described in protocol A. Once the mixture attained room temperature, podophyllotoxone (**1d**, 200 mg, 0.485 mmol) and the ketone or aldehyde (0.97 mmol) were added, and the mixture was maintained under reflux with stirring

during 24 h. The reaction was quenched by addition of 2 N HCl (30 mL), and extraction was with EtOAc. The organic phase was dried with Na_2SO_4, filtered and the solvent removed under reduced pressure. The crude product was purified by flash chromatography with *n*-hexane/EtOAc.

7α-[(1*R*)-1-Hydroxyethyl]-2,2,5-trimethyl-1,3-dioxolan-4-yl)-epipodophyllotoxin Acetonide (4βr) and 7α-[(1*S*)-1-Hydroxyethyl]-2,2,5-trimethyl-1,3-dioxolan-4-yl)epipodophyllotoxin Acetonide (4βs). Following experimental protocol A, **1d** reacted with acetaldehyde (40 μL, 0.91 mmol), yielding 225 mg of reaction crude. Flash chromatography with *n*-hexane/EtOAc (70:30 and 50:50) afforded **1** and **1c**, respectively. Fractions between were dissolved with 2.5 mL of acetone. An amount of 2 mL of 2,2-dimethoxypropane was added, and the mixture was maintained with stirring for 5 min in the presence of some drops of CH_3SiCl. Then it was extracted with EtOAc and washed with $NaHCO_3$, 5%, and water until neutral pH was obtained. The organic solvent was removed, and an amount of 100 mg of reaction crude was obtained. Flash chromatography with *n*-hexane/EtOAc (70:30) afforded compounds **4βr** (30%) and **4βs** (15%). **4βr**: white amorphous powder; mp 128−130 °C; ^{1}H NMR ($CDCl_3$) δ 7.37 (s, 1H), 6.52 (s, 1H), 6.34 (s, 2H), 6.01 (bs, 1H), 5.97 (bs, 1H), 4.61 (d, *J* = 9.7 Hz, 1H), 4.43 (t, *J* = 10 Hz, 1H), 4.37 (t, *J* = 5.7 Hz, 1H), 4.22 (q, *J* = 12.3 Hz, 2H), 3.81 (s, 3H), 3.73 (s, 6H), 3.19 (dd, *J* = 5, 9.6 Hz, 1H), 2.72−2.60 (m, 1H), 1.60 (s, 2H), 1.40 (s, 2H), 1.38 (d, *J* = 13.2 Hz, 2H); ^{13}C NMR ($CDCl_3$) δ 174.8, 152.7 (2C), 147.9, 147.1, 137.1, 134.7, 132.7, 131.4, 109.9, 109.2, 109.0, 107.9 (2C), 101.5, 82.7, 76.6, 67.3, 60.8, 56.1 (2C), 44.2, 43.6, 38.3, 27.3, 25.1, 14.8; $[\alpha]^{22}$ −130° (Na, 589 nm) (*c* 0.5%, EtOH); MS (EI) *m/z* = 498.19 (M^+), 439 (20), 367 (6), 86 (70), 58 (35). HPLC: 97.8%. **4βs**: white amorphous powder; mp 125−128 °C; ^{1}H NMR ($CDCl_3$) δ 7.09 (s, 1H), 6.45 (s, 1H), 6.31 (s, 2H), 5.97 (s, 2H), 4.58 (d, *J* = 5.3 Hz, 1H), 4.54 (t, *J* = 6.1 Hz, 1H), 4.46 (t, *J* = 7.9 Hz, 1H), 4.43 (q, *J* = 10 Hz, 2H), 3.80 (s, 3H), 3.75 (s, 6H), 3.41−3.30 (m, 1H), 2.86 (dd, *J* = 5.7, 15 Hz, 1H), 1.72 (s, 2H), 1.39 (s, 2H), 1.00 (d, *J* = 13.2 Hz, 2H); ^{13}C NMR ($CDCl_3$) δ 173.9, 152.5 (2C), 147.8, 147.1, 137.2, 135.2, 131.6, 131.4, 109.6, 108.4 (2C), 107.9, 107.7, 101.4, 84.5, 74.5, 67.7, 60.8, 56.2 (2C), 44.3, 44.0, 40.4, 27.2, 26.7, 18.9; $[\alpha]^{22}$ −92° (Na, 589 nm) (*c* 1%, EtOH); MS (EI) *m/z* = 498.19 (M^+), 454 (10), 367 (6), 86 (50), 58 (25). HPLC: 97.1%.

7α-[(1*R*)-1-Hydroxybutyl]epipodophyllotoxin (5βr) and 7α-[(1*S*)-1-Hydroxybutyl]epipodophyllotoxin (5βs). Following experimental protocol A, **1d** reacted with butyraldehyde (70 mg, 0.97 mmol), yielding 260 mg of reaction crude. Flash chromatography with *n*-hexane/EtOAc (80:20 and 65:35) afforded compounds **5βr** (30%) and **5βs** (8%). **5βr**: ^{1}H NMR ($CDCl_3$) δ 7.46 (s, 1H), 6.55 (s, 1H), 6.41 (s, 2H), 5.98 (d, *J* = 1.3 Hz, 1H), 5.96 (d, *J* = 1.3 Hz, 1H), 4.57 (d, *J* = 4.8 Hz, 1H), 4.39 (t, *J* = 8.3 Hz, 1H), 4.32 (t, *J* = 7.5 Hz, 1H), 3.90 (m, 1H), 3.80 (s, 3H), 3.73 (s, 6H), 3.22 (dd, *J* = 4.4, 14 Hz, 1H), 3.10−2.90 (m, 1H), 1.69−1.53 (m, 2H), 1.49−1.43 (m, 2H), 0.95 (t, *J* = 6.6 Hz, 3H); ^{13}C NMR ($CDCl_3$) δ 175.0, 152.6 (2C), 148.0, 147.8, 136.8, 134.9, 133.6, 133.5, 110.5, 107.9 (2C), 106.6, 101.6, 76.7, 75.2, 67.7, 60.7, 56.0 (2C), 44.5, 42.4, 37.7, 34.2, 20.4, 14.0; $[\alpha]^{22}$ −47° (Na, 589 nm) (*c* 1.0%, EtOH); IR ν_{max} = 3467, 2934, 1771, 1589, 1506, 1483, 1232, and 1127 cm^{-1}; MS (EI) *m/z* = 468 $(M - 18)^+$, 397, 313, 282, 71. HPLC: 96.5%.

7α-[(1*R*)-1-Cyclohex-3-enyl-1-hydroxymethyl]epipodophyllotoxin (6βr) and 7α-[(1*S*)-1-cyclohex-3-enyl-1-hydroxymethyl]-epipodophyllotoxin (6βs). Following experimental protocol A, **1d** reacted with cyclohex-3-enecarbaldehyde (120 μL, 1.03 mmol), yielding 300 mg of reaction crude. Flash chromatography with *n*-hexane/EtOAc (70:30) afforded compounds **6βr** (38%) and **6βs** (9%). **6βr**: ^{1}H NMR ($CDCl_3$) δ 7.22 (s, 1H), 6.44 (s, 1H), 6.25 (s, 2H), 5.95 (bs, 2H), 5.70 (m, 1H), 5.60 (m, 1H), 4.55 (d, *J* = 5.3 Hz, 1H), 4.49 (m, 1H), 4.35 (m, 1H), 3.78 (s, 3H), 3.70 (s, 7H), 3.09 (m, 1H), 2.80 (dd, *J* = 6, 14 Hz, 1H), 2.15 (m, 1H), 1.95 (m, 1H), 1.70 (m, 1H), 1.45 (m, 1H); ^{13}C NMR ($CDCl_3$) δ 175.1, 152.5 (2C), 147.9, 147.4, 137.1, 133.3, 133.1, 132.4, 127.2, 126.3, 109.9, 108.4 (2C), 107.0, 101.5, 77.7, 77.1, 69.1, 60.8, 56.2 (2C), 44.9, 44.3 (2C), 35.4, 30.8, 25.2, 23.5; $[\alpha]^{22}$ −88° (Na, 589 nm) (*c* 0.5%, EtOH); MS (ES) *m/z* = 547 $[M + Na]^+$. HPLC: 96.0%.

7β-(2-Hydroxyprop-2-yl)podophyllotoxin (7α) and 7α-(2-Hydroxyprop-2-yl)epipodophyllotoxin (7β). Following experimental protocol A, **1d** reacted with acetone in excess, yielding 230 mg of reaction crude. Flash chromatography with *n*-hexane/EtOAc (70:30) afforded compounds **7β** (45%) and **7α** (9%). **7β**: white amorphous powder; mp 142−144 °C; ^{1}H NMR ($CDCl_3$) δ 7.96 (s, 1H), 6.55 (s, 1H), 6.44 (s, 2H), 6.00 (bs, 1H), 5.96 (bs, 1H), 4.58 (d, *J* = 4.8 Hz, 1H), 4.49 (t, *J* = 9 Hz, 1H), 4.44 (t, *J* = 7.9 Hz, 1H), 3.81 (s, 3H), 3.72 (s, 6H), 3.13 (dd, *J* = 4.4, 14 Hz, 1H), 2.70 (m, 1H), 1.27 (s, 4H); ^{13}C NMR ($CDCl_3$) δ 175.2, 152.7 (2C), 147.6, 147.4, 136.9, 135.2, 135.0, 132.1, 109.9, 108.5, 107.8 (2C), 101.5, 78.1 (2C), 69.9, 60.7, 59.8 (2C), 44.2 (2C), 39.2, 28.4, 26.7; IR ν_{max} = 3467, 2934, 1589, 1506, 1483, 1232, and 1127 cm^{-1}; $[\alpha]^{22}$ −150° (Na, 589 nm) (*c* 1,0%, EtOH); EIMS *m/z* = 454 $(M - 18)^+$, 436 (34), 282 (60), 201 (53), 67 (43). HPLC: 98.1%. **7α**: white amorphous powder; mp 116−119 °C; ^{1}H NMR ($CDCl_3$) δ 6.46 (s, 1H), 6.20 (s, 2H), 5.96 (s, 3H), 4.85 (dd, *J* = 9.7, 11 Hz, 1H), 4.61 (d, *J* = 5.7 Hz, 1H), 4.46 (dd, *J* = 7, 9 Hz, 1H), 3.80 (s, 3H), 3.71 (s, 6H), 3.59 (dd, *J* = 5.7, 15 Hz, 1H), 3.05 (m, 1H), 1.49 (s, 2H), 1.31 (s, 2H); ^{13}C NMR ($CDCl_3$) δ 174.8, 152.5 (2C), 148.1, 146.8, 137.1, 135.8, 133.8, 132.2, 110.0, 108.4 (2C), 108.2, 101.5, 78.1, 78.0, 69.6, 60.8, 56.2 (2C), 45.2, 44.7, 44.3, 29.9, 27.5; $[\alpha]^{22}$ −110° (Na, 589 nm) (*c* 0.5%, EtOH); IR ν_{max} = 3467, 2934, 1771, 1789, 1506, 1483, and 1232 cm^{-1}; MS (EI) *m/z* = 454 $(M - 18)^+$, 436 (34), 282 (60), 201 (53), 67 (43). HPLC: 95.2%.

7α-[(2*R*)-2-Hydroxy-3-methylbut-2-yl]epipodophyllotoxin (8βr) and 7α-[(2*S*)-2-Hydroxy-3-methylbut-2-yl]epipodophyllotoxin (8βs). Following experimental protocol A, **1d** reacted with 3-methylbutanone (90 μL, 1.05 mmol), yielding 245 mg of reaction crude. Flash chromatography with *n*-hexane/EtOAc (70:30) afforded compounds **8βr** (45%) and **8βs** (9%). **8βr**: Colorless crystals (CH_2Cl_2); mp 172−174 °C; ^{1}H NMR ($CDCl_3$) δ 8.03 (s, 1H), 6.56 (s, 1H), 6.50 (s, 2H), 6.00 (d, *J* = 1.3 Hz, 1H), 5.95 (d, *J* = 1.3 Hz, 1H), 4.59 (d, *J* = 4.4 Hz, 1H), 4.53 (t, *J* = 10 Hz, 1H), 4.37 (t, *J* = 8.3 Hz, 1H), 3.81 (s, 3H), 3.74 (s, 6H), 3.28 (dd, *J* = 7.6, 12 Hz, 1H), 2.81−2.70 (m, 1H), 2.15−2.10 (m, 1H), 1.16 (s, 3H), 0.93 (d, *J* = 6.6 Hz, 3H), 0.83 (d, *J* = 6.6 Hz, 3H); ^{13}C NMR ($CDCl_3$) δ 175.6, 152.6 (2C), 147.4, 147.1, 137.1, 135.5, 135.4, 132.8, 110.3, 109.3, 108.1 (2C), 101.4, 81.1, 79.1, 68.8, 60.7, 56.1 (2C), 44.4, 44.1, 40.2, 33.0, 21.4, 20.7, 19.0; $[\alpha]^{22}$ −72° (Na, 589 nm) (*c* 1.0%, EtOH); IR ν_{max} = 3467, 2934, 1771, 1589, 1506, 1483, 1232, and 1127 cm^{-1}; MS (EI) *m/z* = 482 $(M - 18)^+$, 439, 367, 282, 55. HPLC: 99.2%. **8βs**: colorless crystals (CH_2Cl_2); mp 169−172 °C; ^{1}H NMR ($CDCl_3$) δ 7.78 (s, 1H), 6.56 (s, 1H), 6.51 (s, 2H), 6.00 (d, *J* = 1.3 Hz, 1H), 5.97 (d, *J* = 1.3 Hz, 1H), 4.57 (d, *J* = 4.4 Hz, 1H), 4.46 (d, *J* = 9.7 Hz, 1H), 3.83 (s, 3H), 3.74 (s, 6H), 3.48 (d, *J* = 7 Hz, 1H), 3.14 (dd, *J* = 4.4, 14 Hz, 1H), 2.91−2.80 (m, 1H), 2.72 (m, 1H), 1.87 (m, 3H), 1.01 (d, *J* = 6.6 Hz, 3H), 0.82 (d, *J* = 6.6 Hz, 3H); ^{13}C NMR ($CDCl_3$) δ 175.2, 152.7 (2C), 147.6, 147.5, 136.0, 135.0 (2C), 132.9, 110.2, 108.4, 108.0 (2C), 101.6, 80.6, 80.5, 69.3, 60.8, 56.1 (2C), 44.3 (2C), 39.4, 34.4, 22.7, 19.8, 18.3; $[\alpha]^{22}$ −69° (Na, 589 nm) (*c* 0.5%, EtOH); IR ν_{max} = 3467, 2934, 1771, 1589, 1506, 1483, 1232, and 1127 cm^{-1}; MS (EI) *m/z* = 482 $(M - 18)^+$, 271, 229, 185, 115. HPLC: 97.1%.

8βr and (*E*)-7-(3-Methyl-2-butylidene)deoxypodophyllotoxin (21). Following experimental protocol B, **1d** reacted with 3-methylbutanone (90 μL, 1.05 mmol) to yield 240 mg of reaction crude. Flash chromatography with *n*-hexane/EtOAc (80:20 and 70:30) afforded **8βr** (14%) and **21** (47%). **8βr** has been described above. **21**: colorless crystals; mp 142−144 °C; ^{1}H NMR ($CDCl_3$) δ 6.87 (s, 1H), 6.65 (s, 1H), 6.36 (s, 2H), 5.97 (bs, 2H), 4.69 (dd, *J* = 6.6, 8.3 Hz, 1H), 4.53 (d, *J* = 3.5 Hz, 1H), 4.09 (dd, *J* = 8.3, 11 Hz, 1H), 3.80 (s, 3H), 3.72 (s, 6H), 3.45−3.30 (m, 1H), 3.25−3.10 (m, 1H), 2.77 (dd, *J* = 3.5, 15 Hz, 1H), 1.63 (s, 3H), 1.14 (d, *J* = 6.6 Hz, 3H), 0.98 (d, *J* = 6.6 Hz, 3H); ^{13}C NMR ($CDCl_3$) δ 174.1, 152.9 (2C), 146.4, 146.0, 141.4, 137.1 (2C), 134.6, 130.5, 127.2, 110.0 (2C), 107.0 (2C), 101.3, 71.3, 60.8, 56.2 (2C), 50.8, 45.0, 41.1, 31.5, 21.7, 20.9, 14.9; $[\alpha]^{22}$ −58° (Na, 589 nm) (*c* 1.0%, EtOH); EIMS *m/z* = 466 (M^+), 435, 379, 283, 165, 153. HPLC: 96.3%.

7α-[(1*R*)-1-Hydroxy-1-(3,4-dimethoxyphenyl)ethyl]-epipodophyllotoxin (9βr). Following experimental protocol A, **1d** reacted with 1-(3,4-dimethoxyphenyl)ethanone (176.5 mg, 0.97 mmol),

yielding 350 mg of reaction crude. Flash chromatography with *n*-hexane/EtOAc (40:60) afforded compound **9βr** (30%). Yellow amorphous powder; mp 163−165 °C; ^{1}H NMR ($CDCl_3$) δ 7.45 (s, 1H), 6.74−6.66 (m, 2H), 6.42 (s, 1H), 6.14 (s, 2H), 5.99 (bs, 2H), 5.61−5.55 (m, 1H), 4.92 (t, *J* = 9.7 Hz, 1H), 4.35 (t, *J* = 8.8 Hz, 1H), 4.13 (d, *J* = 6 Hz, 1H), 3.86 (s, 3H), 3.75 (s, 6H), 3.69 (s, 6H), 3.48 (dd, *J* = 1.8; 6.6 Hz, 1H), 2.97−2.94 (m, 1H), 1.72 (s, 3H); ^{13}C NMR ($CDCl_3$) δ 175.0, 152.3 (2C), 148.3, 148.3, 146.6, 136.9, 136.2 (2C), 135.6, 134.7, 131.9, 110.5, 109.8 (2C), 108.2 (3C), 107.9, 101.6, 80.3, 78.1, 69.0, 60.7, 56.2 (3C), 55.7, 45.5, 44.5, 42.5, 30.8; $[\alpha]^{22}$ −75° (Na, 589 nm) (*c* 1.0%, EtOH); MS (ES) *m/z* = 617.20 [M + Na]$^+$, 536 (40), 331 (20), 149 (35). HPLC: 98.5%.

7α-[(1*R*)-1-Hydroxy-2-methyl-1-phenylpropyl]epipodophyllotoxin (10β) and (*E*)-7-(2-Methyl-1-phenyl-1-propylidene)-deoxypodophyllotoxin (22). Following experimental protocol B, **1d** reacted with 2-methyl-1-phenylpropan-1-one (150 μL, 1.0 mmol), yielding 340 mg of reaction crude. Flash chromatography with *n*-hexane/EtOAc (80:20, 70:30, and 60:40) afforded compounds **22** (40%) and **10β** (15%). **22**: colorless crystals (CH_2Cl_2); mp 165−166 °C; ^{1}H NMR ($CDCl_3$) δ 7.45−7.40 (m, 2H), 7.23−7.19 (m, 2H), 6.69 (d, *J* = 7.5 Hz, 1H), 6.59 (s, 1H), 6.53 (s, 2H), 6.12 (s, 1H), 5.80 (d, *J* = 1.3 Hz, 1H), 5.77 (d, *J* = 1.3 Hz, 1H), 4.76 (t, *J* = 8.3 Hz, 1H), 4.55 (d, *J* = 3.1 Hz, 1H), 4.17 (dd, *J* = 8; 1.8 Hz, 1H), 3.84 (s, 9H), 3.44−3.41 (m, 2H), 3.35 (dd, *J* = 3, 11.9 Hz, 1H), 2.96 (m, 1H), 1.18 (d, *J* = 7 Hz, 3H), 0.65 (d, *J* = 6.6 Hz, 3H); ^{13}C NMR ($CDCl_3$) δ 174.0, 153.0 (2C), 147.5, 146.0, 145.5, 139.9, 137.1, 135.2, 130.5 (2C), 129.7, 128.7 (2C), 128.2, 127.1, 126.9, 111.5, 109.2, 106.6 (2C), 101.0, 71.9, 60.8, 56.2 (2C), 50.3, 45.0, 40.0, 32.4, 22.7, 20.6; $[\alpha]^{22}$ +150° (Na, 589 nm) (*c* 1.0%, EtOH); MS (ES) *m/z* = 551.20 [M + Na]$^+$. HPLC: 96.0%. **10β**: colorless crystals; mp 115−118 °C; ^{1}H NMR ($CDCl_3$) δ 7.92 (s, 1H), 7.29 (m, 2H), 7.24−7.13 (m, 3H), 6.45 (s, 1H), 6.27 (s, 2H), 5.96 (d, *J* = 1.3 Hz, 1H), 5.93 (d, *J* = 1.3 Hz, 1H), 4.41 (d, *J* = 4.4 Hz, 1H), 4.37 (m, 1H), 3.84 (s, 3H), 3.75 (s, 1H), 3.69 (s, 6H), 3.23−3.21 (m, 1H), 3.05 (dd, *J* = 4.4, 8.8 Hz, 1H), 2.48−2.44 (m, 1H), 0.98 (d, *J* = 6.1 Hz, 3H), 0.92 (d, *J* = 7 Hz, 3H); ^{13}C NMR ($CDCl_3$) δ 175.4, 152.6 (2C), 147.1, 146.9, 141.4, 137.4, 135.3, 134.3, 133.5, 127.6 (2C), 127.0, 126.9, 110.2, 109.1, 108.8 (2C), 101.4, 82.6, 82.1, 70.0, 60.7, 56.6 (2C), 44.3, 44.0, 39.8, 36.8, 19.2, 18.7; $[\alpha]^{22}$ −143° (Na, 589 nm) (*c* 1.0%, EtOH); MS (ES) *m/z* = 585.21 [M + Na]$^+$. HPLC: 96.3%.

7β-(1-Hydroxy-1,1-diphenylmethyl)podophyllotoxin (11α) and 7α-(1-Hydroxy-1,1-diphenylmethyl)epipodophyllotoxin (11β). Following experimental protocol A, **1d** reacted with benzophenone (178.5 mg, 0,97 mmol), yielding 365 mg of reaction crude. Flash chromatography with *n*-hexane/EtOAc (70:30) afforded compounds **11β** (35%) and **11α** (5%). **11β**: colorless crystals (CH_2Cl_2); mp 168−170 °C; ^{1}H NMR ($CDCl_3$) δ 7.94 (bs, 2H), 7.77 (dd, *J* = 2.2, 6.6 Hz, 4H), 7.38−7.29 (m, 6H), 7.29 (s, 1H), 6.55 (s, 2H), 6.53 (s, 1H), 5.87 (d, *J* = 1.3 Hz, 1H), 5.81 (d, *J* = 1.3 Hz, 1H), 4.45 (bs, 1H), 3.95 (m, 1H), 3.84 (s, 10H), 3.13 (dd, *J* = 1.8, 3.5 Hz, 1H), 2.52 (bs, 1H); ^{13}C NMR ($CDCl_3$) δ 175.0, 152.6 (2C), 147.9, 147.1, 145.4, 143.6, 137.4, 135.2, 134.5, 133.5, 128.6 (2C), 128.3, 127.7 (2C), 126.8 (5C), 110.9, 108.8 (2C), 107.2, 101.6, 82.6, 80.8, 68.5, 60.7, 56.5 (2C), 44.9, 43.0, 40.5; $[\alpha]^{22}$ −100° (Na, 589 nm) (*c* 1.0%, EtOH); MS (EI) *m/z* = 619.19 [M + Na]$^+$, 605 (20), 308 (30), 217 (30). HPLC: 96.0%. **11α**: white amorphous powder; mp 163−165 °C; ^{1}H NMR ($CDCl_3$) δ 7.58−7.56 (m, 2H), 7.48−7.39 (m, 2H), 7.38−7.32 (m, 6H), 6.46 (s, 1H), 6.20 (s, 2H), 5.90 (d, *J* = 1.3 Hz, 1H), 5.82 (d, *J* = 1.3 Hz, 1H), 5.66 (s, 1H), 4.48 (t, *J* = 7 Hz, 1H), 4.44 (d, *J* = 5.7 Hz, 1H), 3.76 (s, 3H), 3.72 (s, 6H), 3.48 (t, *J* = 8 Hz, 1H), 3.12 (dd, *J* = 3.8; 10 Hz, 1H), 2.45 (m, 1H); ^{13}C NMR ($CDCl_3$) δ 174.8, 152.3 (2C), 148.2, 146.3, 143.0, 139.9, 138.0, 135.5, 134.3, 131.1, 128.8, 128.5, 128.2, 128.1, 127.2 (3C), 126.8, 126.3, 125.6, 109.6, 108.2 (3C), 101.4, 83.7 (2C), 79.7, 69.1, 60.7, 56.1 (2C), 45.9, 43.4; $[\alpha]^{22}$ −40° (Na, 589 nm) (*c* 0.5%, EtOH); MS (EI) *m/z* = 619.19 [M + Na]$^+$, 605 (20), 308 (30), 217 (30). HPLC: 96.4%.

7α-(1-Hydroxycyclobutyl)epipodophyllotoxin (12β). Following experimental protocol A, **1d** reacted with cyclobutanone (67.9 mg, 0.97 mmol), yielding 260 mg of reaction crude. Flash chromatography with *n*-hexane/EtOAc (60:40) afforded compound **12β** (40%). **12β**: colorless crystals (CH_2Cl_2); mp 168−170 °C; ^{1}H NMR ($CDCl_3$) δ 6.96 (s, 1H), 6.56 (s, 1H), 6.46 (s, 2H), 5.97 (s, 2H), 4.50 (d, *J* = 4.4 Hz, 1H), 4.40 (t, *J* = 8 Hz, 1H), 4.28 (t, *J* = 7 Hz, 1H), 3.80 (s, 3H), 3.74 (s, 6H), 3.23−3.14 (m, 1H), 3.10 (dd, *J* = 4.4, 14 Hz, 1H), 2.33−2.05 (m, 4H), 1.89−1.69 (m, 2H); ^{13}C NMR ($CDCl_3$) δ 174.9, 152.7 (2C), 148.0, 147.7, 136.8, 134.6 (2C), 133.6, 110.8, 108.1 (2C), 105.2, 101.6, 83.1, 75.8, 68.2, 60.7, 56.1 (2C), 44.7, 42.5, 37.5, 33.0, 30.9, 15.8; $[\alpha]^{22}$ −47° (Na, 589 nm) (*c* 1.0%, EtOH); IR ν_{max} = 3467, 2934, 1771, 1689, 1506, 1232, and 1127 cm^{-1}; MS (EI) *m/z* = 466 (M − 18)$^+$, 410, 242, 207, 168, 55. HPLC: 96.5%.

7β-(1-Hydroxycyclopentyl)podophyllotoxin (13α) and 7α-(1-hydroxycyclopentyl)epipodophyllotoxin (13β). Following experimental protocol A, **1d** reacted with cyclopentanone (80 μL, 0.95 mmol), yielding 250 mg of reaction crude. Flash chromatography with *n*-hexane/EtOAc (60:40) afforded compounds **13β** (40%) and **13α** (8%). **13β**: White amorphous powder; mp 117−119 °C; ^{1}H NMR ($CDCl_3$) δ 7.78 (s, 1H), 6.55 (s, 1H), 6.49 (s, 2H), 6.00 (d, *J* = 1.3 Hz, 1H), 5.57 (d, *J* = 1.3 Hz, 1H), 4.57 (d, *J* = 4.4 Hz, 1H), 4.50 (t, *J* = 7.5 Hz, 1H), 4.45 (t, *J* = 5.3 Hz, 1H), 3.82 (s, 3H), 3.73 (s, 6H), 3.15 (dd, *J* = 4, 11.8 Hz, 1H), 2.90−2.85 (m, 1H), 1.85−1.55 (m, 8H); ^{13}C NMR ($CDCl_3$) δ 175.3, 152.6 (2C), 147.6, 147.3, 136.7, 135.5, 135.0, 133.3, 110.0, 108.3, 107.8 (2C), 101.6, 83.3, 77.7, 69.2, 60.8, 56.0 (2C), 44.5, 44.0, 39.6, 37.6, 36.6, 23.7, 22.4; $[\alpha]^{22}$ −87° (Na, 589 nm) (*c* 1.0%, EtOH); MS (EI) *m/z* = 480 (M − 18)$^+$, 282, 207, 133, 73. HPLC: 96.7%. **13α**: white amorphous powder; mp 120−121 °C; ^{1}H NMR ($CDCl_3$) δ 7.24 (s, 1H), 6.45 (s, 1H), 6.19 (s, 2H), 5.96 (bs, 2H), 4.65 (m, 1H), 4.55 (m, 1H), 4.45 (m, 1H), 3.79 (s, 3H), 3.73 (s, 6H), 3.65 (m, 1H), 3.05−2.90 (m, 1H), 1.80−1.54 (m, 4H); ^{13}C NMR ($CDCl_3$) δ 174.9, 152.5 (2C), 148.0, 146.5, 137.1, 136.1, 133.8, 132.3, 110.0, 108.3 (2C), 108.2, 101.5, 88.5, 78.1, 69.7, 60.8, 56.2 (2C), 45.9, 44.5, 43.5, 37.2, 35.7, 22.3, 21.4; $[\alpha]^{22}$ −188° (Na, 589 nm) (*c* 0.5%, EtOH); MS (EI) *m/z* = 480 (M − 18)$^+$, 282, 207, 133, 73. HPLC: 95.2%.

7β-(1-Hydroxycyclohexyl)podophyllotoxin (14α) and 7α-(1-Hydroxycyclohexyl)epipodophyllotoxin (14β). Following experimental protocol A, **1d** reacted with cyclohexanone (100 μL, 0.97 mmol), yielding 280 mg of reaction crude. Flash chromatography with *n*-hexane/EtOAc (60:40) afforded compounds **14β** (40%) and **14α** (7%). **14β**: colorless crystals ($CDCl_3$); mp 106−108 °C; ^{1}H NMR ($CDCl_3$) δ 7.95 (s, 1H), 6.52 (s, 1H), 6.44 (s, 2H), 5.98 (d, *J* = 1.6 Hz, 1H), 5.94 (d, *J* = 1.6 Hz, 1H), 4.54 (d, *J* = 4,4 Hz, 1H), 4.50 (t, *J* = 10 Hz, 1H), 4.42 (t, *J* = 8 Hz, 1H), 3.80 (s, 3H), 3.73 (s, 6H), 3.13 (dd, *J* = 4; 13.6 Hz, 1H), 2.63 (ddd, *J* = 3, 6, 11 Hz, 1H), 1.68−1.55 (m, 4H), 1.28−1.20 (m, 4H), 1.07−1.02 (m, 2H); ^{13}C NMR ($CDCl_3$) δ 175.2, 152.6 (2C), 147.4, 147.3, 136.8, 135.1 (2C), 133.2, 109.8, 108.9, 107.7 (2C), 101.4, 78.7, 77.8, 69.2, 60.7, 56.8 (2C), 44.5, 44.1, 39.1, 34.5, 33.0, 25.2, 21.7, 21.3; $[\alpha]^{22}$ −190° (Na, 589 nm) (*c* 1.0%, EtOH); IR ν_{max} = 3502, 2934, 1772, 1589, 1506, 1483, 1232, and 1128 cm^{-1}; MS (ES) *m/z* = 535.19 [M + Na]$^+$, 530 (85), 477 (35), 399 (30). HPLC: 99.1%. **14α**: white amorphous powder; mp 102−104 °C; ^{1}H NMR ($CDCl_3$) δ 7.08 (s, 1H), 6.51 (s, 1H), 6.40 (s, 2H), 5.96 (d, *J* = 2.4 Hz, 1H), 5.93 (d, *J* = 2.4 Hz, 1H), 4.42 (d, *J* = 4.8 Hz, 1H), 4.28 (t, *J* = 8.8 Hz, 1H), 3.78 (s, 3H), 3.71 (s, 6H), 3.50 (dd, *J* = 4.8; 12.8 Hz, 1H), 3.46 (dd, *J* = 5, 9.6 Hz, 1H), 2.95−2.85 (m, 1H), 1.76−1.66 (m, 4H), 1.43 (m, 4H), 0.95−0.85 (m, 2H); ^{13}C NMR ($CDCl_3$) δ 175.7, 152.7 (2C), 147.5, 147.3, 136.7, 135.4, 132.7, 129.9, 108.5, 106.7 (2C), 106.3, 101.2, 88.0, 82.3, 68.3, 60.7, 56.0 (2C), 50.6, 48.3, 45.4, 31.4, 31.3, 25.6, 22.9, 21.5; $[\alpha]^{22}$ −110° (Na, 589 nm) (*c* 0.5%, EtOH); IR ν_{max} = 3467, 2934, 1771, 1589, 1506, 1483, 1232, and 1127 cm^{-1}; MS, *m/z* (%) = 494 (M − 18)$^+$, 367 (34), 282 (60), 201 (53), 67 (43). HPLC: 95.1%.

7α-(1-Hydroxycyclohexyl)epipicropododophylloxin (14βp). To a solution of 30 mg of compound **14β** (0.07 mmol) in 3 mL of methanol, an amount of 3 mL of KOH (5%) in methanol was added. The mixture was maintained with stirring for 30 min at room temperature. Then the solvent was removed, water was added and neutralized with HCl, 2 N, and finally extracted with EtOAc. After the organic phase was washed with an aqueous solution saturated with NaCl, it was dried with Na_2SO_4. After removal of the solvent,

compound **14βp** (67%) was obtained. White amorphous powder; mp 110−113 °C; ^{1}H NMR ($CDCl_3$) δ 7.20 (s, 1H), 6.48 (s, 3H), 5.98 (d, *J* = 1.3 Hz, 1H), 5.94 (d, *J* = 1.3 Hz, 1H), 4.43 (dd, *J* = 7.5, 9 Hz, 1H), 4.26 (d, *J* = 6 Hz, 1H), 4.04 (t, *J* = 9.6 Hz, 1H), 3.84 (s, 3H), 3.77 (s, 6H), 3.45 (q, *J* = 7.9 Hz, 1H), 3.10 (m, 1H), 1.60−1.36 (m, 10H); ^{13}C NMR ($CDCl_3$) δ 179.6, 153.1 (2C), 147.4, 146.7, 136.7, 140.9, 130.3, 129.2, 109.5, 105.7 (2C), 108.1, 101.3, 77.6, 76.8, 70.8, 60.8, 56.1 (2C), 46.2, 42.9, 41.1, 32.6, 32.4, 21.6 (2C), 25.3; $[\alpha]^{22}$ +63° (Na, 589 nm) (*c* 0.5%, EtOH); IR ν_{max} = 3467, 2934, 1771, 1589, 1506, 1483, 1232, and 1127 cm^{-1}; MS (EI) *m/z* = 494 (M − 18)$^+$, 367 (34), 282 (60), 201 (53), 67 (43). HPLC: 98.2%.

7β-(9-Hydroxybicyclo[3.3.1]non-9-yl)podophyllotoxin (15α) and 7α-(9-Hydroxybicyclo[3.3.1]non-9-yl)epipodophyllotoxin (15β). Following experimental protocol A, **1d** reacted with bicycle[3:3:1]nonan-9-one (132 mg, 0.96 mmol), yielding 325 mg of reaction crude. Flash chromatography with *n*-hexane/EtOAc (70:30) afforded compounds **15β** (30%) and **15α** (20%). **15β**: white amorphous powder; mp 118−120 °C; ^{1}H NMR ($CDCl_3$) δ 7.32 (s, 3H), 6.43 (s, 1H), 5.98 (d, *J* = 1.3 Hz, 1H), 5.95 (d, *J* = 1.3 Hz, 1H), 4.60 (dd, *J* = 9, 9 Hz, 1H), 4.60 (d, *J* = 7 Hz, 1H), 4.45 (dd, *J* = 4, 9 Hz, 1H), 3.79 (s, 3H), 3.74 (s, 6H), 3.10 (m, 1H), 2.75 (m, 1H), 2.45−2.20 (m, 2H), 2.05−1.85 (m, 8H), 1.55−1.45 (m, 2H), 1.35−1.25 (m, 2H); ^{13}C NMR ($CDCl_3$) δ 175.0, 152.5 (2C), 147.9, 146.7, 137.3, 136.7, 133.8, 133.0, 110.5, 108.4 (2C), 107.7, 101.5, 80.6, 79.5, 69.4, 60.8, 56.3 (2C), 47.3, 45.0, 42.6, 35.3, 34.3, 30.0, 29.3, 29.2, 28.6, 20.1, 19.2; $[\alpha]^{22}$ −88° (Na, 589 nm) (*c* 1.0%, EtOH); IR ν_{max} = 3467, 2934, 1771, 1589, 1506, 1483, 1232, and 1127 cm^{-1}; MS (ES) *m/z* = 575.23 [M + Na]$^+$. HPLC: 96.8%. **15α**: white amorphous powder; mp 126−128 °C; ^{1}H NMR ($CDCl_3$) δ 7.24 (s, 1H), 6.78 (s, 2H), 6.64 (s, 1H), 6.01 (d, *J* = 2.2 Hz, 1H), 5.99 (d, *J* = 2.2 Hz, 1H), 4.51 (d, *J* = 4 Hz, 1H), 4.48 (t, *J* = 5.3 Hz, 1H), 4.43 (t, *J* = 4.8 Hz, 1H), 3.83 (s, 3H), 3.79 (s, 6H), 3.43−3.35 (m, 2H), 2.85 (dd, *J* = 4.4, 14 Hz, 1H), 2.55 (m, 1H), 2.15−1.90 (m, 6H), 1.70−1.45 (m, 6H); ^{13}C NMR ($CDCl_3$) δ 174.6, 152.5 (2C), 147.6, 146.8, 136.8, 135.5 (2C), 133.9, 110.7, 108.3 (3C), 101.6, 84.0, 77.6, 69.9, 60.7, 56.2 (2C), 45.3, 44.7, 40.0, 35.6, 35.4, 30.4, 29.6, 29.1, 28.3, 20.4, 20.0; $[\alpha]^{22}$ −53° (Na, 589 nm) (*c* 1.0%, EtOH); IR ν_{max} = 3467, 2934, 1771, 1589, 1506, 1483, 1232, and 1127 cm-^{1}; MS (ES) *m/z* = 575.23 [M + Na]$^+$. HPLC: 95.4%.

7β-(4-Hydroxytetrahydropyran-4-yl)podophyllotoxin (16α) and 7α-(4-Hydroxytetrahydropyran-4-yl)epipodophyllotoxin (16β). Following experimental protocol A, **1d** reacted with tetrahydropyran-4-one (97 mg, 0.97 mmol) to yield 280 mg of reaction crude. Flash chromatography with *n*-hexane/EtOAc, 30:70, afforded **16β** (38%) and **16α** (15%). **16β**: white amorphous powder; mp 210−213 °C; ^{1}H NMR ($CDCl_3$) δ 7.84 (s, 1H), 6.47 (s, 1H), 6.38 (s, 2H), 5.92 (bs, 2H), 4.51 (d, *J* = 4.4 Hz, 1H), 4.43 (dd, *J* = 2.6; 12 Hz, 1H), 3.74 (s, 3H), 3.73 (m, 1H), 3.65 (s, 6H), 3.12 (dd, *J* = 3.9, 13.6 Hz, 1H), 1.60 (m, 4H), 1.38 (m, 2H), 1.15 (m, 2H); ^{13}C NMR ($CDCl_3$) δ 175.7, 152.5 (2C), 147.4, 147.0, 136.5, 135.1, 134.0, 133.2, 109.7, 109.1, 107.6 (2C), 101.4, 78.1, 74.9, 69.3, 63.5, 63.3, 60.6, 56.8 (2C), 44.3, 44.1, 39.2, 35.1, 33.2; IR ν_{max} 3467, 2934, 1771, 1589, 1506, 1483, 1232, and 1127 cm^{-1}; $[\alpha]^{22}$ −108° (Na, 589 nm) (*c* 1.0%, EtOH); MS (ES) *m/z* = 537,17 ([M + Na]$^+$). HPLC: 96.5%. **16α**: colorless crystals; mp 170−173 °C; ^{1}H NMR ($CDCl_3$) δ 7.08 (s, 1H), 6.51 (s, 1H), 6.43 (bs, 2H), 5.93 (bs, 2H), 4.40 (bs, 1H), 4.36 (m, 1H), 3.93 (m, 1H), 3.69 (bs, 9H), 3.07 (m, 1H), 3.06−2.89 (m, 4H), 2.20−2.10 (m, 1H), 1.29−1.24 (m, 4H); ^{13}C NMR ($CDCl_3$) δ 177.0, 152.5 (2C), 147.6, 147.5, 136.4, 136.1, 132.9, 129.5, 108.6, 106.9 (2C), 106.5, 101.3, 85.9, 81.7, 68.9, 65.3, 63.2, 60.6, 56.0 (3C), 51.2, 48.4, 46.0, 32.2; IR ν_{max} 3467, 2934, 1771, 1589, 1506, 1483, 1232, and 1127 cm^{-1}; $[\alpha]^{22}$ −36° (Na, 589 nm) (*c* 1.0%, EtOH); MS (ES) *m/z* = 537.17 ([M + Na]$^+$). HPLC: 95.2%.

7α-(4-Hydroxytetrahydrothiopyran-4-yl)epipodophyllotoxin (17β). Following experimental protocol A, **1d** reacted with tetrahydrothiopyran-4-one (123 mg, 0.97 mmol), yielding 320 mg of reaction crude. Flash chromatography with *n*-hexane/EtOAc, 20:80, afforded compound **17β** (15%). White amorphous powder; mp 198−201 °C; ^{1}H NMR ($CDCl_3$) δ 7.97 (s, 1H), 6.57 (s, 1H), 6.42 (s, 2H), 6.02 (s, 1H), 5.99 (s, 1H), 4.59 (d, *J* = 4.4 Hz, 1H), 4.48 (t, *J* = 5.7 Hz, 1H), 4.45 (m, 1H), 3.84 (s, 3H), 3.73 (s, 6H), 3.13 (dd, *J* = 4, 4.4 Hz, 1H), 2.51 (dd, *J* = 3.5, 10.5 Hz, 1H), 1.60−1.50 (m, 4H), 0.95−0.75 (m, 4H); MS (ES) *m/z* = 553.15 [M + Na]$^+$. HPLC: 96.1%.

7-Methylidenedeoxypodophyllotoxin (18). **18** was prepared from **1d** (300 mg) as described in ref 33. Flash chromatography with *n*-hexane/EtOAc, 80:20, afforded **18** (180 mg, 60%). The spectral data (IR, ^{1}H NMR, and ^{13}C NMR) were comparable with the data reported in the same reference. HPLC: 97.0%.

7-(2-Propylidene)desoxypodophyllotoxin (19). Following experimental protocol B, **1d** reacted with acetone in excess, yielding 220 mg of reaction crude. Flash chromatography with *n*-hexane/EtOAc, 80:20 and 70:30, afforded **19** (46%) and **7β** (15%). **19**: yellowish oil; ^{1}H NMR ($CDCl_3$) δ 6.94 (s, 1H), 6.66 (s, 1H), 6.34 (s, 2H), 5.99 (bs, 2H), 4.69 (t, *J* = 7 Hz, 1H), 4.56 (d, *J* = 3.5 Hz, 1H), 4.12 (dd, *J* = 7.9, 11 Hz, 1H), 3.81 (s, 3H), 3.72 (s, 6H), 3.17 (m, 1H), 2.81 (dd, *J* = 3.5, 14.7 Hz, 1H), 2.08 (s, 2H), 1.81 (s, 2H); ^{13}C NMR ($CDCl_3$) δ 174.0, 152.7 (2C), 146.2, 145.9, 136.7, 134.5, 134.4, 131.6, 130.8, 127.2, 110.6, 109.7, 106.5 (2C), 101.2, 71.2, 60.7, 58.9 (2C), 50.4, 44.8, 40.6, 24.7, 23.7; $[\alpha]^{22}$ −130° (Na, 589 nm) (*c* 0.5%, EtOH); EIMS *m/z* (%) = 438 (M$^+$), 270 (20), 225 (50), 181 (26), 152 (25). HPLC: 97.1%. **7β** has been described above.

7α-Isopropyldeoxypodophyllotoxin (20). Compound **19** (22 mg, 0.05 mmol) in EtOH (5 mL) in the presence of a catalytic amount of Pd/C was maintained with stirring at room temperature under hydrogen during 36 h. After filtration and solvent removing, compound **20** (95%) was obtained. Pale yellow oil; ^{1}H NMR ($CDCl_3$) δ 6.91 (s, 1H), 6.53 (s, 1H), 6.44 (s, 2H), 5.98 (d, *J* = 1.3 Hz, 1H), 5.95 (d, *J* = 1.3 Hz, 1H), 4.58 (t, *J* = 6.6 Hz, 1H), 4.54 (d, *J* = 3.5 Hz, 1H), 3.97 (dd, *J* = 10.2, 8.8 Hz, 1H), 3.81 (s, 3H), 3.73 (s, 6H), 2.95 (dd, *J* = 3.6, 10.2 Hz, 1H), 2.78 (dd, *J* = 13.9, 4.4 Hz, 1H), 2.57 (m, 1H), 1.05 (d, *J* = 7 Hz, 3H), 0.85 (d, *J* = 6.6 Hz, 3H); ^{13}C NMR ($CDCl_3$) δ 175.1, 152.5 (2C), 147.5, 146.4, 136.7, 136.1, 132.8, 132.0, 110.4, 108.0 (2C), 106.7, 101.3, 73.0, 60.7, 56.0 (2C), 49.9, 47.3, 44.2, 32.9, 31.4, 21.7, 17.1; $[\alpha]^{22}$ −91° (Na, 589 nm) (*c* 1.0%, EtOH); EIMS *m/z* = 440 (M$^+$), 313 (20), 282 (50), 209 (37). HPLC: 97.6%.

Cytotoxicity Assays. A-549 (ATCC CCL-185) (lung carcinoma), HT-29 (ATCC HTB-38), (colorectal carcinoma), and SK-BR3 (ATCC HTB-30) (breast adenocarcinoma) cell lines were obtained from the ATCC. Cell lines were maintained in RPMI medium supplemented with 10% fetal calf serum (FCS), 2 mM L-glutamine, and 100 U/mL penicillin and streptomycin at 37 °C and 5% CO_2. Tumor cells were incubated for 72 h in the presence or absence of test compounds (10 different concentrations ranging from 10 to 0.0026 μg/mL). For quantitative estimation of cytotoxicity, the colorimetric sulforhodamine B (SRB) method was used, essentially performed as described previously.[35a] Briefly, cells were washed twice with PBS, fixed for 15 min in 1% glutaraldehyde solution, rinsed twice in PBS, and stained in 0.4% SRB solution for 30 min at room temperature. Cells were then rinsed several times with 1% acetic acid solution and air-dried. Sulforhodamine B was then extracted in 10 mM Trizma base solution and the absorbance measured at 490 nm. Results are expressed as GI_{50}, the compound concentration that causes 50% inhibition in cell growth compared to control cell growth (NCI algorithm).[35b] The relative activity of each compound was calculated from dose−response curves generated with the results from triplicate parallel cultures.

Cell Cycle Analysis. Progression through the cell cycle was assessed by flow cytometry DNA determination with propidium iodide. Cells (180 000 per mL) were incubated with several concentrations of the compounds or drugs for 20 h. The cells were fixed with 70% ethanol, treated with RNase, and stained with propidium iodide as previously described.[45] Analysis was with a Coulter Epics XL flow cytometer.

Tubulin Assembly. Purified calf brain tubulin and chemicals were as previously described.[46] Ligands were dissolved in DMSO-d_6 at 20 mM and kept at −80 °C. Work solutions were done in DMSO and kept at −20 °C. The 50% inhibitory ligand concentration of tubulin assembly was determined with a centrifugation assay. Tubulin was equilibrated prior to use in 3.4 M glycerol, 1 mM EGTA, 0.1 mM

GTP, pH 7.0, buffer through a 25 cm × 0.9 cm Sephadex G-25 column. Aggregates were removed by a centrifugation at 90000*g* × 10 min in a TLA120 rotor at 4 °C in an Optima TLX centrifuge. Tubulin concentration was determined spectrophotometrically using an extinction coefficient of 107 000 M^{-1} cm^{-1} at 275 nm in 10 mM phosphate buffer and 1% SDS, employing a Thermo Evolution 300 LC spectrophotometer and adjusting to 20 μM.[47] Tubulin was kept at 4 °C, and 0.9 mM GTP and 6 mM $MgCl_2$ were added to the sample. The solution was distributed in 200 μL polycarbonate tubes for the TL100 rotor. Growing concentrations of the ligands ranging from 0 to 25 μM were added to the samples (DMSO content of the samples, 2.5%), which were incubated for 30 min at 37 °C. Microtubules were separated from unassembled tubulin by a centrifugation at 90000*g* × 10 min in a TLA100 rotor at 37 °C in an Optima TLX centrifuge. The supernatant containing unassembled tubulin was carefully collected and the microtubule pellet resuspended in 10 mM sodium phosphate buffer, pH 7.0, containing 1% SDS. Both supernatants and pellets were diluted 1:5 in the same buffer, and tubulin concentrations were measured fluorometrically (λ_{exc} = 280; λ_{ems} = 323) using tubulin standards calibrated spectrophotometrically. The 50% inhibitory ligand concentration of tubulin assembly was determined with a centrifugation assay that measured the decrease in the concentrations of microtubules assembled in the presence of different concentrations of the compound or reference drug.

Ligand Binding to Tubulin. The effect of compounds **1a**, **16α**, and **20** in the binding of 2-methoxy-5-(2,3,4-trimethoxyphenyl)-2,4,6-cycloheptatrien-1-one MTC[48] was studied as described.[49,50]

Cell Culture and Indirect Inmunofluorescence. Human non-small-cell lung carcinoma A-549 cells were continuously maintained in RPMI-1640 supplemented with 10% fetal calf serum, 2 mM L-glutamine, 40 μg/mL gentamycin, 100 IU/mL penicillin, and 100 μg/mL streptomycin. A-549 human lung carcinoma cells were plated at a density of 150 000 cells/ml onto 24-well tissue culture plates containing 12 mm round coverslips, cultured overnight, and then treated with ligands at different concentrations or drug vehicle (DMSO) for 24 h. Residual DMSO was less than 0.5%. Attached cells were permeabilized with Triton X100 and fixed with 3.7% formaldehyde, as previously described.[51] Cytoskeletons were incubated with DM1A monoclonal antibody reacting with α-tubulin, washed twice, and incubated with FITC goat anti-mouse immunoglobulins. The coverslips were washed, and 1 μg/mL Hoechst 33342 to stain chromatin was added. The mixture was incubated for 30 min. After the samples were washed, they were examined and photographed using a Zeiss Axioplan epifluorescence microscope. The images were recorded with a Hamamatsu 4742-95 cooled CCD camera.

■ ASSOCIATED CONTENT

Supporting Information

^{1}H and ^{13}C NMR spectra of selected compounds, quantitative analytical data, supplementary cytotoxicity data, cell cycle effects, tubulin polymerization inhibition, and pictures of effects on microtubule array of cancer cells. This material is available free of charge via the Internet at http://pubs.acs.org.

■ AUTHOR INFORMATION

Corresponding Author

*For J.L.L.-P.: phone, +34-923-294528; fax, +34-923-294515; e-mail, lopez@usal.es. For J.F.D.: phone, +34-91-8373112, e-mail, fer@cib.csic.es.

Notes

The authors declare no competing financial interest.

■ ACKNOWLEDGMENTS

A.A. is thankful for the fellowship and facilities of Universidad de los Andes, Mérida, Venezuela. Financial support came from the Spanish "Ministerio de Sanidad y Consumo-ISCIII" (Grant PI060782), "Ministerio de Ciencia e Innovación" (Grant BIO2010-16351 to J.F.D.), and "Junta de Castilla y León" (Grant SAO30A06).

■ REFERENCES

(1) (a) Newman, D. J.; Cragg, G. M.; Snader, K. M. Natural products as sources of new drugs over the period 1981−2002. *J. Nat. Prod.* **2003**, *66*, 1022−1037. (b) Newman, D. J. Natural products as leads to potential drugs: an old process or the new hope for drug discovery. *J. Med. Chem.* **2008**, *51*, 2589−2599.

(2) (a) Butler, M. S. Natural products to drugs: natural product derived compounds in clinical trials. *Nat. Prod. Rep.* **2005**, *22*, 162−195. (b) Butler, M. S. Natural products to drugs: natural product-derived compounds in clinical trials. *Nat. Prod. Rep.* **2008**, *25*, 475−516.

(3) Butler, M. S. A Snapshot of Natural Product-Derived Compounds in Late Stage Clinical Development at the End of 2008. In *Natural Product Chemistry for Drug Discovery*; Buss, A. D., Butler, M. S., Eds; RSC: Cambridge, U.K., 2010; pp 321−354.

(4) Hartwell, J. L.; Schrecker, A. W. The chemistry of podophyllum. *Fortschr. Chem. Org. Naturst.* **1958**, *15*, 83−166.

(5) Imbert, T. F. Discovery of podophyllotoxins. *Biochimie* **1998**, *80*, 207−222.

(6) Schacter, L. Etoposide phosphate: what, why, where, and how? *Semin. Oncol* **1996**, *23*, 23−7.

(7) (a) Stahelin, H.; von Wartburg, A. From podophyllotoxin glucoside to etoposide. *Prog. Drug Res.* **1989**, *33*, 169−266. (b) Stahelin, H. F.; von Wartburg, A. The chemical and biological route from podophyllotoxin glucoside to etoposide: Ninth Cain Memorial Award Lecture. *Cancer Res.* **1991**, *51*, 5−15.

(8) Kluza, J.; Mazinghien, R.; Irwin, H.; Hartley, J. A.; Bailly, C. Relationships between DNA strand breakage and apoptotic progression upon treatment of HL-60 leukemia cells with tafluposide or etoposide. *Anti-Cancer Drugs* **2006**, *17*, 155−164.

(9) VanVliet, D. S.; Tachibana, Y.; Bastow, K. F.; Huang, E. S.; Lee, K. H. Antitumor agents. 207. Design, synthesis, and biological testing of 4beta-anilino-2-fluoro-4′-demethylpodophyllotoxin analogues as cytotoxic and antiviral agents. *J. Med. Chem.* **2001**, *44*, 1422−1428.

(10) Clinical Trials. http://clinicaltrials.gov/ct2/results?term=etoposide (893 study references found by May 2, 2011).

(11) Rassmann, I.; Thodtmann, R.; Mross, M.; Huttmann, A.; Berdel, W. E.; Manegold, C.; Fiebig, H. H.; Kaeser-Frohlich, A.; Burk, K.; Hanauske, A. R. Phase I clinical and pharmacokinetic trial of the podophyllotoxin derivative NK611 administered as intravenous short infusion. *Invest. New Drugs* **1998**, *16*, 319−324.

(12) Moss, G. P. Nomenclature of lignans and neolignans. *Pure Appl. Chem.* **2000**, *72*, 1493−1523.

(13) Chang, H.; Shyu, K. G.; Lee, C. C.; Tsai, S. C.; Wang, B. W.; Hsien Lee, Y.; Lin, S. GL331 inhibits HIF-1alpha expression in a lung cancer model. *Biochem. Biophys. Res. Commun.* **2003**, *302*, 95−100.

(14) Zhu, X. K.; Guan, J.; Tachibana, Y.; Bastow, K. F.; Cho, S. J.; Cheng, H. H.; Cheng, Y. C.; Gurwith, M.; Lee, K. H. Antitumor agents. 194. Synthesis and biological evaluations of 4-beta-mono-, -di-, and -trisubstituted aniline-4′-*O*-demethyl-podophyllotoxin and related compounds with improved pharmacological profiles. *J. Med. Chem.* **1999**, *42*, 2441−2446.

(15) Huang, T. S.; Lee, C. C.; Chao, Y.; Shu, C. H.; Chen, L. T.; Chen, L. L.; Chen, M. H.; Yuan, C. C.; Whang-Peng, J. A novel podophyllotoxin-derived compound GL331 is more potent than its congener VP-16 in killing refractory cancer cells. *Pharm. Res.* **1999**, *16*, 997−1002.

(16) Liu, Y. Q.; Yang, L.; Tian, X. Podophyllotoxin: current perspectives. *Curr. Bioact. Compd.* **2007**, *3*, 37−66.

(17) Zhu, X. K.; Guan, J.; Xiao, Z.; Cosentino, L. M.; Lee, K. H. Anti-AIDS agents. Part 61: anti-HIV activity of new podophyllotoxin derivatives. *Bioorg. Med. Chem.* **2004**, *12*, 4267−4273.

(18) Gordaliza, M.; Faircloth, G. T.; Castro, M. A.; Miguel del Corral, J. M.; López-Vázquez, M. L.; San Feliciano, A. Immunosuppressive cyclolignans. *J. Med. Chem.* **1996**, *39*, 2865−2868.

(19) Dumontet, C.; Jordan, M. A. Microtubule-binding agents: a dynamic field of cancer therapeutics. *Nat. Rev. Drug Discovery* **2010**, *9*, 790−803.

(20) (a) Jordan, A.; Hadfield, J. A.; Lawrence, N. J.; McGown, A. T. Tubulin as a target for anticancer drugs: agents which interact with the mitotic spindle. *Med. Res. Rev.* **1998**, *18*, 259−296. (b) Hande, K. R. Etoposide: four decades of development of a topoisomerase II inhibitor. *Eur. J. Cancer* **1998**, *34*, 1514−1521. (c) Meresse, P.; Dechaux, E.; Monneret, C.; Bertounesque, E. Etoposide: discovery and medicinal chemistry. *Curr. Med. Chem.* **2004**, *11*, 2443−2466. (d) You, Y. Podophyllotoxin derivatives: current synthetic approaches for new anticancer agents. *Curr. Pharm. Des.* **2005**, *11*, 1695−1717.

(21) Castro, M. A.; del Corral, J. M.; García, P. A.; Rojo, M. V.; de la Iglesia-Vicente, J.; Mollinedo, F.; Cuevas, C.; San Feliciano, A. Synthesis and biological evaluation of new podophyllic aldehyde derivatives with cytotoxic and apoptosis-inducing activities. *J. Med. Chem.* **2010**, *53*, 983−993.

(22) Mukherjee, A. K.; Basu, S.; Sarkar, N.; Ghosh, A. C. Advances in cancer therapy with plant based natural products. *Curr. Med. Chem.* **2001**, *8*, 1467−1486.

(23) Gupta, S.; Das, L.; Datta, A. B.; Poddar, A.; Janik, M. E.; Bhattacharyya, B. Oxalone and lactone moieties of podophyllotoxin exhibit properties of both the B and C rings of colchicine in its binding with tubulin. *Biochemistry* **2006**, *45*, 6467−6475.

(24) Kim do, Y.; Kim, K. H.; Kim, N. D.; Lee, K. Y.; Han, C. K.; Yoon, J. H.; Moon, S. K.; Lee, S. S.; Seong, B. L. Design and biological evaluation of novel tubulin inhibitors as antimitotic agents using a pharmacophore binding model with tubulin. *J. Med. Chem.* **2006**, *49*, 5664−5670.

(25) Xiao, Z.; Bastow, K. F.; Vance, J. R.; Lee, K. H. Antitumor agents. Part 227: studies on novel 4′-*O*-demethyl-epipodophyllotoxins as antitumor agents targeting topoisomerase II. *Bioorg. Med. Chem.* **2004**, *12*, 3339−3344.

(26) Xiao, Z.; Xiao, Y. D.; Feng, J.; Golbraikh, A.; Tropsha, A.; Lee, K. H. Antitumor agents. 213. Modeling of epipodophyllotoxin derivatives using variable selection *k* nearest neighbor QSAR method. *J. Med. Chem.* **2002**, *45*, 2294−2309.

(27) Chatterjee, A.; Joshi, N. N. Evolution of the stereoselective pinacol coupling reaction. *Tetrahedron* **2006**, *62*, 12137−12158.

(28) López-Pérez, J. L.; Abad, A.; del Olmo, E.; San Feliciano, A. Correct structures of Diels−Alder adducts from the natural cyclolignan thuriferic acid and its 8-epimer. *Tetrahedron* **2006**, *62*, 2370−2379.

(29) McMurry, J. E. Carbonyl-coupling reactions using low-valent titanium. *Chem. Rev.* **1989**, *89*, 1513−1524.

(30) Ephritikhine, M. A new look at the McMurry reaction. *Chem. Commun.* **1998**, 2549−2554.

(31) Dyker, G.; Korning, J.; Stirner, W. Synthesis and photocyclization of macrocyclic stilbene derivatives. *Eur. J. Org. Chem.* **1998**, 149−154.

(32) Höfert, P. H.; Matusch, R. A novel rearrangement product of podophyllotoxone-ester derivates and in vitro cytotoxicity studies. *Helv. Chim. Acta* **1994**, *77*, 771−777.

(33) Roulland, E.; Magiatis, P.; Arimondo, P.; Bertounesque, E.; Monneret, C. Hemi-synthesis and biological activity of new analogues of podophyllotoxin. *Bioorg. Med. Chem.* **2002**, *10*, 3463−3471.

(34) López-Pérez, J. L.; Theron, R.; del Olmo, E.; Díaz, D. NAPROC-13: a database for the dereplication of natural product mixtures in bioassay-guided protocols. *Bioinformatics* **2007**, *23*, 3256−3257.

(35) (a) Vichai, V.; Kirtikara, K. Sulforhodamine B colorimetric assay for cytotoxicity screening. *Nat. Protoc.* **2006**, *1*, 1112−1116. (b) Boyd, M. R.; Paull, K. D. Some practical considerations and applications of the National Cancer Institute in vitro anticancer drug discovery screen. *Drug Dev. Res.* **1995**, *34*, 91−109.

(36) Sackett, D. L. Podophyllotoxin, steganacin and combretastatin: natural products that bind at the colchicine site of tubulin. *Pharmacol. Ther.* **1993**, *59*, 163−228.

(37) Gordaliza, M.; Castro, M. A.; García-Grávalos, M. D.; Ruiz, P.; Miguel del Corral, J. M.; San Feliciano, A. Antineoplastic and antiviral activities of podophyllotoxin related lignans. *Arch. Pharm. (Weinheim, Ger.)* **1994**, *327*, 175−179.

(38) Jordan, M. A.; Thrower, D.; Wilson, L. Effects of vinblastine, podophyllotoxin and nocodazole on mitotic spindles. Implications for the role of microtubule dynamics in mitosis. *J. Cell Sci.* **1992**, *102*, 401−416.

(39) Fitzgerald, T. J. Molecular features of colchicine associated with antimitotic activity and inhibition of tubulin polymerization. *Biochem. Pharmacol.* **1976**, *25*, 1383−1387.

(40) Medrano, F. J.; Andreu, J. M.; Gorbunoff, M. J.; Timasheff, S. N. Roles of ring C oxygens in the binding of colchicine to tubulin. *Biochemistry* **1991**, *30*, 3770−3777.

(41) Álvarez, C.; Álvarez, R.; Corchete, P.; López, J. L.; Pérez-Melero, C.; Peláez, R.; Medarde, M. Diarylmethyloxime and hydrazone derivatives with 5-indolyl moieties as potent inhibitors of tubulin polymerization. *Bioorg. Med. Chem.* **2008**, *16*, 5952−5961.

(42) Ravelli, R. B.; Gigant, B.; Curmi, P. A.; Jourdain, I.; Lachkar, S.; Sobel, A.; Knossow, M. Insight into tubulin regulation from a complex with colchicine and a stathmin-like domain. *Nature* **2004**, *428*, 198−202.

(43) (a) *Spartan 08*; Wavefunction, Inc.: Irvine, CA. (b) Hehre, W. J. *A Guide to Molecular Mechanics and Quantum Chemical Calculations*; Wavefunction, Inc.: Irvine, CA, 2003.

(44) Huey, R.; Morris, G. M.; Olson, A. J.; Goodsell, D. S. A semiempirical free energy force field with charge-based desolvation. *J. Comput. Chem.* **2007**, *28*, 1145−1152.

(45) Andreu, J. M.; Barasoain, I. The interaction of baccatin III with the Taxol binding site of microtubules determined by a homogeneous assay with fluorescent taxoid. *Biochemistry* **2001**, *40*, 11975−11984.

(46) (a) Diaz, J. F.; Andreu, J. M. Assembly of purified GDP-tubulin into microtubules induced by Taxol and Taxotere: reversibility, ligand stoichiometry, and competition. *Biochemistry* **1993**, *32*, 2747−2755. (b) Andreu, J. M. Large Scale Purification of Tubulin from Brain Employing the Modified Weisengerg Procedure. In *Microtubule Protocols*; Zhou, J., Ed.; Methods in Molecular Medicine, Vol. *137*; Humana Press Inc.: Totowa, NJ, 2007; pp 17−28.

(47) Andreu, J. M.; Gorbunoff, M. J.; Lee, J. C.; Timasheff, S. N. Interaction of tubulin with bifunctional colchicine analogues: an equilibrium study. *Biochemistry* **1984**, *23*, 1742−1752.

(48) Fitzgerald, T. J. Molecular features of colchicine associated with antimitotic activity and inhibition of tubulin polymerization. *Biochem. Pharmacol.* **1976**, *25*, 1383−1387.

(49) Andreu, J. M.; Pérez-Ramírez, B.; Gorbunoff, M. J.; Ayala, D.; Timasheff, S. N. Role of the colchicine ring A and its methoxy groups in the binding to tubulin and microtubule inhibition. *Biochemistry* **1998**, *37*, 8356−8368.

(50) La Regina, G.; Edler, M. C.; Brancale, A.; Kandil, S.; Coluccia, A.; Piscitelli, F.; Hamel, E.; De Martino, G.; Matesanz, R.; Diaz, J. F.; Scovassi, A. I.; Prosperi, E.; Lavecchia, A.; Novellino, E.; Artico, M.; Silvestri, R. Arylthioindole inhibitors of tubulin polymerization. 3. Biological evaluation, structure−activity relationships and molecular modeling studies. *J. Med. Chem.* **2007**, *50*, 2865−2874.

(51) De Ines, C.; Leynadier, D.; Barasoain, I.; Peyrot, V.; Garcia, P.; Briand, C.; Rener, G. A.; Temple, C., Jr. Inhibition of microtubules and cell cycle arrest by a new 1-deaza-7,8-dihydropteridine antitumor drug, CI 980, and by its chiral isomer, NSC 613863. *Cancer Res.* **1994**, *54*, 75−84.